Spatial patterns in abundance, taxonomic composition and carbon biomass of nano- and microphytoplankton in Subarctic and Arctic Seas

David W. Crawford[a], Adrián O. Cefarelli[a,c], Ian A. Wrohan[b], Shea N. Wyatt[a], Diana E. Varela[a,b,*]

[a] Department of Biology, University of Victoria, Victoria, British Columbia V8W 2Y2, Canada
[b] School of Earth and Ocean Sciences, University of Victoria, Victoria, British Columbia V8W 2Y2, Canada
[c] Centro de Investigaciones y Transferencia Golfo San Jorge, Consejo Nacional de Investigaciones Científicas y Técnicas, 9000 Comodoro Rivadavia, Chubut, Argentina

ARTICLE INFO

ABSTRACT

In the summers of 2007 and 2008, we studied assemblages of nano- and microphytoplankton from the subsurface chlorophyll maximum (SCM) across five broad oceanographic domains in the seas surrounding northern North America. These domains are the eastern Subarctic North Pacific (ESNP), Bering and Chukchi Seas (BE-CH), Beaufort Sea and Canada Basin (BS-CB), Canadian Arctic Archipelago (CAA), and Baffin Bay and Labrador Sea (BB-LS). Average abundance and total carbon biomass (C) of phytoplankton ($> 2\ \mu m$) varied ~10-fold and ~20-fold, respectively, across the five domains. In the BE-CH, CAA and BB-LS, diatoms averaged 35–70% and dinoflagellates 11–45% of total phytoplankton C ($> 2\ \mu m$), whereas in the ESNP and BS-CB, unidentified flagellates/coccoids (2–$8\ \mu m$) represented a greater proportion of total C (27% and 39% respectively) than in the other domains.

In the BE-CH and BB-LS, phytoplankton C ($> 2\ \mu m$) was dominated by dinoflagellates of the genus *Gymnodinium*, centric diatoms including *Thalassiosira* spp. and *Chaetoceros* spp., unidentified flagellates/coccoids (2–$8\ \mu m$), and cryptomonads. In contrast, diatoms such as *Thalassiosira* spp. and its resting spores dominated C in the CAA, with dinoflagellates being less significant than in the BE-CH and BB-LS. Unidentified flagellates/coccoids (2–$8\ \mu m$), *Gymnodinium* spp., and cryptomonads dominated in the ESNP, and particularly in the BS-CB, where diatoms contributed only 18% of the very low levels of total phytoplankton C ($> 2\ \mu m$).

Phytoplankton C ($> 2\ \mu m$) to chlorophyll *a* ratios (phyto C:chl *a*) averaged only $31\ g\ C\ g\ chl\ a^{-1}$ in the oligotrophic BS-CB domain, and 51–$150\ g\ C\ g\ chl\ a^{-1}$ in the other domains, whereas ratios of biogenic silica to phytoplankton C ($> 2\ \mu m$) (bSi:phyto C) were lowest in the eastern domains. Estimates of phytoplankton C were highly sensitive to the choice of C to cell volume equations (C:vol) adopted in the calculations, particularly in diatom-rich areas.

This study highlights how diatoms and dinoflagellates are the main drivers of large-scale variations in C biomass for phytoplankton ($> 2\ \mu m$), whereas unidentified flagellates/coccoids (2–$8\ \mu m$) make a significant contribution to C biomass in oligotrophic domains, such as BS-CB, where diatoms and dinoflagellates are less abundant. Reduced surface water density (σ_T) was associated with deeper SCM layers, and with decreased C biomass of unidentified flagellates/coccoids (2–$8\ \mu m$). These observations confirm recent studies highlighting the role of surface water stratification caused by melting sea ice in shaping nano- and microphytoplankton assemblages.

1. Introduction

Recent enhanced melting of sea ice has exposed greater areas of the Arctic Ocean to wind stress, irradiance and freshening of surface waters, resulting in increased coastal productivity in some areas (Tremblay et al., 2011), and latitudinal shifts of biological boundaries in others (Grebmeier et al., 2006). In the stratified southeast Beaufort Sea, seasonal nitrate (NO_3^-) consumption and net community production (NCP) increased between 2003 and 2011, but decreased in the North Water Polynya in northern Baffin Bay between 1997 and 2011 as a result of increasing surface freshening and stratification (Bergeron and Tremblay, 2014). In the Canada Basin, a gradual deepening of the subsurface chlorophyll maximum (SCM) has led to a shift in the size composition of the phytoplankton assemblages (Li et al., 2009). With these rapidly changing oceanographic conditions in the Arctic and Subarctic, there is a pressing need to understand how large-scale
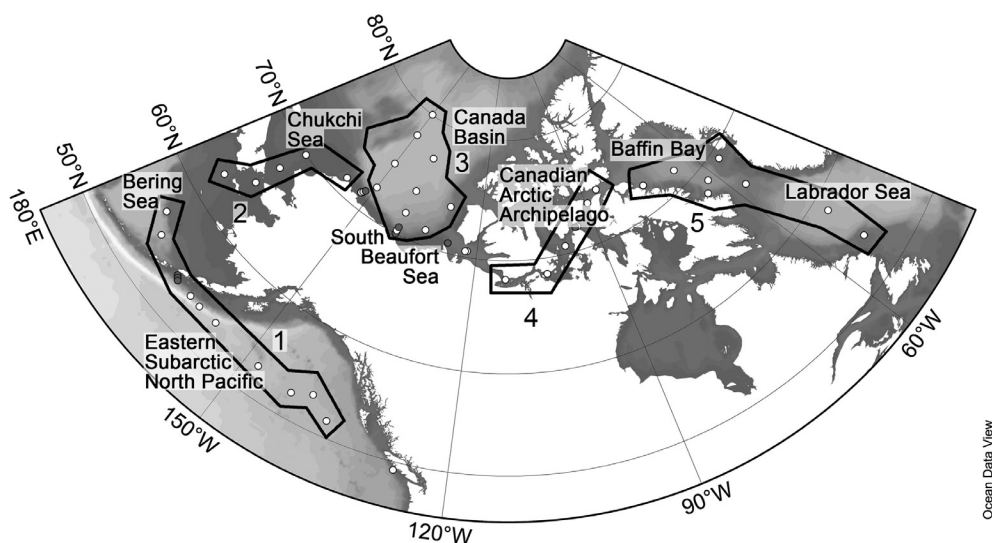
Fig. 1. Study areas in Arctic and Subarctic Seas around northern North America showing the sampling stations during summers of 2007 (eastern sector and Canada Basin; C3O/JOIS cruises) and 2008 (western sector; C3O cruise). See Section 2.1 and Tables 1 and 2 for details of regions sampled during each cruise. White circles represent full-profile sampling stations where phytoplankton samples were taken from the depth of the subsurface chlorophyll maximum (SCM). Grey circles represent surface stations where phytoplankton samples were taken from depths of 2–10 m. For further cruise details see Carmack and McLaughlin (2011), Varela et al. (2013) and Wyatt et al. (2013). The oceanographic domains consist of (1) the Eastern Subarctic North Pacific Ocean (ESNP), (2) the Bering and Chukchi Seas (BE-CH), (3) the Beaufort Sea and Canada Basin (BS-CB), (4) the Canadian Arctic Archipelago (CAA), and (5) Baffin Bay and Labrador Sea (BB-LS). Station markers shown outside of these domains represent excluded stations (see Table 1).

physical and chemical changes will shift biological communities in the future. The Arctic has traditionally been a challenging environment to study but improvements in technology, ship access and availability of historical datasets are promoting more synoptic oceanographic studies on physical processes (e.g. Carmack and McLaughlin, 2011), nutrient cycling (e.g. Codispoti et al., 2013), primary productivity (e.g. Ardyna et al., 2011; Hill et al., 2013; Matrai et al., 2013; Varela et al., 2013; Hill et al., 2017) and the composition of suspended biogenic particles (e.g. Wyatt et al., 2013; Crawford et al., 2015).

Limited light penetration and lack of wind action due to sea-ice cover in the deep Arctic basins result in an upper water column characterized by low irradiance and low nutrient concentrations, with phytoplankton assemblages consequently limited in biomass and productivity (e.g. Varela et al., 2013). Under these oligotrophic conditions, phytoplankton often aggregate within a distinct SCM where nutrient availability is optimized at light levels still adequate for photosynthesis (Martin et al., 2012). Seasonal thinning and melting of sea ice can promote phytoplankton productivity by exposing a greater sea surface area to irradiance and wind forcing over shallow shelves (Tremblay et al., 2011), whereas in deeper basins melting can reduce productivity by enhancing the strong density stratification that inhibits vertical supply of nutrients (McLaughlin and Carmack, 2010). The Arctic Ocean is also an advective estuarine environment (Carmack and Wassmann, 2006; Yamamoto-Kawai et al., 2006) where chemical and biological changes in one area can transform the lateral supply of nutrients to other areas (e.g. Tremblay et al., 2002).

Research on pelagic and sea-ice unicellular autotrophs in Arctic marine waters extends back to the late 1800s (e.g. see review by Poulin et al., 2011). For much of the 20th century descriptive studies focused primarily on taxonomic examinations of larger cells that could be readily collected and preserved (Poulin et al., 2011), but later studies began to address how phytoplankton assemblages are shaped by physical and chemical processes in Arctic and Subarctic waters (e.g. Booth, 1988; Booth and Horner, 1997; Booth and Smith, 1997). Analyses of the composition of phytoplankton assemblages are subject to particular drawbacks that hamper large-scale studies. Painstaking microscopic examination is highly skilled and labour intensive, limiting the sampling resolution achievable in oceanographic surveys. Changing taxonomic nomenclature can also potentially complicate comparisons with historical studies. The methodology employed for sampling and preserving phytoplankton has resulted in a historical bias towards microphytoplankton (20–200 μm), although there is now an increasing interest in the role of nanophytoplankton (2–20 μm) and picophytoplankton (0.2–2 μm) in the Arctic Ocean (e.g. Li et al., 2009; Tremblay et al., 2009; Ardyna et al., 2011), particularly in open

oligotrophic regions where heterotrophic protists are also clearly important (e.g. Sherr et al., 1997; Kirchman et al., 2009). Separation of autotrophic carbon (C) from heterotrophic and detrital C is challenging using light microscopy (Booth, 1987) and consequently, other methods have been increasingly used to evaluate the importance of smaller autotrophs, such as fluorescence microscopy (Booth, 1987), chemotaxonomic analyses of pigments (Vidussi et al., 2004; Hill et al., 2005; Tremblay et al., 2009; Coupel et al., 2012; Coupel et al., 2015) and flow cytometry (Li et al., 2009; Tremblay et al., 2009; Ardyna et al., 2011; Balzano et al., 2012). Molecular techniques such as 18S rRNA gene are also being used on both autotrophic and heterotrophic protists (Lovejoy et al., 2011; Lovejoy and Potvin, 2011). The presence of sea-ice unicellular autotrophs in close proximity to phytoplankton assemblages (e.g. Gosselin et al., 1997), and the aggregation of phytoplankton within discrete SCM layers are also potential complications in the accuracy of sampling and enumeration of phytoplankton assemblages in the vertical dimension. Despite these drawbacks, some large-scale surveys of Arctic phytoplankton assemblages are now emerging, both in the form of extensive literature reviews (e.g. Poulin et al., 2011) and long oceanographic transects (Gosselin et al., 1997; Tremblay et al., 2009; Ardyna et al., 2011).

The International Polar Year (IPY) Canada Three Oceans (C3O) project undertaken during the summers of 2007 and 2008, combined with the ongoing Joint Ocean Ice Study (JOIS) project, provided an opportunity to compare phytoplankton assemblages across the Arctic and Subarctic Seas surrounding northern North America. In the present study, we used the domain classification of Carmack and McLaughlin (2011), which was already applied to contrast large-scale variations in physical oceanography (Carmack and McLaughlin, 2011), primary productivity and nutrient uptake (Varela et al., 2013), and composition of biogenic particles (Wyatt et al., 2013; Crawford et al., 2015). This investigation complements these previous studies by comparing the abundance, C biomass and taxonomy of nano- and microphytoplankton within the SCM among domains during the summer period.

2. Methods

2.1. Study area and domain classification

Seawater samples were collected across the northwest Atlantic, Arctic, and northeast Pacific Oceans (Fig. 1). The sampling stations were arranged into five broad-scale regional domains that coincide with distinct water masses revealed by temperature/salinity (T/S) correlations (Carmack and McLaughlin, 2011). These domains (Fig. 1, Table 1) consist of the Eastern Subarctic North Pacific Ocean (ESNP), the Bering

Table 1

Oceanographic domains and stations for cruises 2007–19, 2007–20, and 2008–02 in the summers of 2007 and 2008, operated by the Institute of Ocean Sciences, Fisheries and Oceans Canada (see Varela et al., 2013 for more details). Phytoplankton samples were taken from the subsurface chlorophyll maximum (SCM), where present, or from the depth indicated where no SCM was present. At surface only stations (*), the depth of the SCM was unknown, and samples were taken from a depth of between 2 and 10 m (~50% surface irradiance). Excluded stations represent those that could not be included in any of the five broad regional domains defined according to oceanographic properties by Carmack and McLaughlin (2011).

Domain	Cruise	Station	Lat (°N)	Long (°W)	Date	Depth of sample collection at SCM (m)	% Ice cover
BB-LS	2007–19	LS-2	54.253	54.100	7 July 2007	15	0
		LS-4	58.489	53.662	8 July 2007	5	0
		LS-7	66.000	57.673	10 July 2007	15	30
		BB-1	69.195	56.422	11 July 2007	2	0
		BB-5	68.831	61.760	12 July 2007	5	90
		BB-8	68.085	64.006	12 July 2007	40	90
		BB-10	71.566	65.401	14 July 2007	5	70
		BEW-11	72.385	73.894	16 July 2007	5	100
CAA	2007–19	CAA-2	74.218	85.646	17 July 2007	40	10
		CAA-5	73.525	89.511	20 July 2007	54	0
		CAA-6	71.949	94.289	22 July 2007	10	100
		CAA-10	70.651	98.589	23 July 2007	37	100
		CAA-12	68.673	103.916	24 July 2007	55	90
		CAA-16	68.382	113.114	25 July 2007	30	0
		BE-2*	72.006	94.586	21 July 2007	Surface only*	
BS-CB	2007–20	BI-2	73.824	129.199	30 July 2007	85	80
		CB-29	71.992	140.040	31 July 2007	64	80
		CB-2a	72.499	150.045	4 August 2007	10	100
		CB-4	74.920	150.147	6 August 2007	46	100
		CB-9	77.935	149.826	9 August 2007	49	100
		CB-11b	79.989	150.012	12 August 2007	63	100
		CB-15	76.999	140.187	14 August 2007	63	100
		CB-21	73.967	140.088	23 August 2007	74	90
		MK-3*	70.582	140.048	1 August 2007	Surface only*	
		MK-1*	70.230	140.004	1 August 2007	Surface only*	
		CB-28aa*	70.003	140.010	2 August 2007	Surface only*	
		BL-4*	71.502	151.657	4 August 2007	Surface only*	
	2008–02	MK-1	70.230	140.004	25 July 2008	97	0
		BFB-5	71.333	133.748	26 July 2008	44	80
		BFB-6*	70.826	127.424	26 July 2008	Surface only*	
BE-CH	2008–02	SLIP-4	63.026	173.456	16 July 2008	30	0
		UTBS1	64.990	169.140	17 July 2008	6	0
		UTN-4	67.504	168.903	19 July 2008	25 (no SCM)	0
		CCL-4	69.991	168.020	20 July 2008	8	60
		BC-2	71.414	157.497	21 July 2008	18	70
ESNP	2008–02	NP-5	51.645	136.659	5 July 2008	5	0
		NP-6	53.489	139.762	6 July 2008	35	0
		NP-8	52.620	142.476	7 July 2008	31	0
		NP-9	53.095	148.052	8 July 2008	36	0
		NP-12	53.712	156.125	10 July 2008	20	0
		NP-13	53.702	159.292	10 July 2008	3	0
		NP-14	53.743	161.110	11 July 2008	21	0
		BCL-2	55.061	170.216	15 July 2008	15	0
		BS-5	56.652	172.735	14 July 2008	33	0
		UN-7*	53.734	163.931	11 July 2008	Surface only*	
		UN-4*	53.960	164.333	11 July 2008	Surface only*	
		UN-2*	54.112	164.581	11 July 2008	Surface only*	
Excluded stations	2007–20	AG-5	70.547	122.898	28 July 2007	12	0
		BL-2	71.402	152.047	3 August 2007	38	10
		BL-1*	71.325	152.218	3 August 2007	Surface only*	
	2008–02	NP-1	49.119	126.691	3 July 2008	5	0
		BL-1	71.324	152.212	23 July 2008	22 (no SCM)	20
		BFB-7	70.545	122.545	27 July 2008	43	0

* Denotes surface station only, where samples were taken from 2 to 10 m depth. No associated vertical profiles or ice cover estimates were taken at these surface stations by Varela et al. (2013) or Wyatt et al. (2013) and the depth of the SCM was unknown.

and Chukchi Seas (BE-CH), the South Beaufort Sea (off shelf) and Canada Basin (BS-CB), the Canadian Arctic Archipelago (CAA), and Baffin Bay and Labrador Sea (BB-LS).

We present phytoplankton data from the same stations as those described in Varela et al. (2013), Wyatt et al. (2013) and Crawford et al. (2015), with the exceptions of 5 stations that were not sampled for phytoplankton taxonomy (full-profile station RS-1 in the BS-CB domain,

and surface stations BC-4, BCL-6, BS-3, BS-1 in the BE-CH domain). In addition, several stations were excluded from the domain classification (Table 1, see also Varela et al., 2013) because they were located in transitional zones where physical conditions were not consistent with neighbouring domains (Carmack and McLaughlin, 2011; Varela et al., 2013).

2.2. Sampling program

Sampling started in the Labrador Sea in early July 2007 aboard the CCGS Louis S. St-Laurent (C3O cruise 2007-19) and continued through Baffin Bay and the Canadian Arctic Archipelago (Fig. 1 and Table 1; see also Varela et al., 2013). During the subsequent JOIS cruise (2007–20) in July–August 2007, still aboard the CCGS Louis S. St-Laurent, sampling was carried out in the southern Beaufort Sea (off shelf) and Canada Basin. The July 2008 C3O cruise (2008-02), aboard the CCGS Sir Wilfrid Laurier, sampled from the west coast of Vancouver Island (Canada), through the northeast Pacific, the Bering Sea, Chukchi Sea, and southern Beaufort Sea (off shelf).

Throughout all cruises, consistent methodologies were adopted for sampling, enumeration of phytoplankton taxa, and all calculations. Station identification and positions are presented in Table 1, and a fuller account of background data for all stations is given in Table 1 of Varela et al. (2013). Complementary physical information, and chemical and biological samples were collected at the same stations, consisting of full-profile stations (sampled from the surface to the bottom of the euphotic zone) and surface stations (only one surface depth sampled); data and methodologies are presented elsewhere (Carmack and McLaughlin, 2011; Varela et al., 2013; Wyatt et al., 2013; Crawford et al., 2015). Mean properties for each domain are summarized from these studies in Table 2. The chlorophyll data used in the present study refer to total chl a ($> 0.7\,\mu m$) as given in Varela et al. (2013). Density

of seawater is presented as σ_T (kg m^{-3} – 1000). Stratification index was calculated as the difference in σ_T between the surface and the depth of 1% surface irradiance. The use of a fixed lower depth of e.g. 80 m (e.g. Ardyna et al., 2011) for this calculation was precluded by the shallow water encountered in some areas, such as the BE-CH. However, the index is relatively insensitive to the choice of lower depth because most of the stratification of σ_T occurs within the upper $\sim 30\,m$ (see Fig. 2).

Samples for nano- and microphytoplankton analyses from full-profile stations were collected from the depth of the SCM where present (Table 1). When the SCM was absent, samples were taken at depths shown in Table 1. At an additional 10 stations, full vertical profiles were not taken and "surface" only samples were collected at 2–10 m depth (within the surface mixed layer where present), which typically corresponded to the depth of 50% of incident surface irradiance. The depth of the SCM was therefore unknown at these "surface" stations; phytoplankton data derived from these stations are included in the raw counts shown in the Appendix Tables 1–6, but are not included in station distribution data and domain averages (Figs. 3–7) which refer only to samples from the SCM.

2.3. Identification and enumeration of phytoplankton taxa

On the ship, water samples were taken using Niskin bottles, and subsamples were preserved with Lugol's iodine solution (Parsons et al., 1984) for identification and enumeration of phytoplankton taxa. In the

Table 2

Physical, chemical and biological properties of the water column for the five oceanographic domains, summarized from data presented by Varela et al. (2013). Measurements for each variable are domain averages for the "surface" (2–10 m) and for the depth of the subsurface chlorophyll maximum (SCM). Data from full-profile stations only. Standard error in parentheses.

		ESNP	BE-CH	BS-CB	CAA	BB-LS
Number of stations		9	5	10	6	8
Ice cover (%)		0	26.0 (16.0)	83.0 (9.7)	50.0 (21.0)	47.5 (15.8)
Depth of SCM (m)		22.11 (4.20)	17.40 (4.66)	58.10 (7.73)	37.67 (6.82)	11.50 (4.42)
Depth of 1% surface Irradiance (m)		46.50 (7.15)	26.40 (3.08)	60.90 (7.48)	35.83 (2.61)	35.71 (2.77)
Temperature (°C)	Surface	9.13 (0.39)	3.76 (0.70)	1.21 (1.04)	2.11 (1.00)	1.76 (1.11)
	SCM	7.57 (0.49)	0.79 (0.97)	-0.22 (0.72)	-1.16 (0.20)	0.87 (1.10)
Salinity	Surface	32.47 (0.09)	31.26 (0.64)	24.07 (1.00)	28.79 (0.72)	31.83 (0.51)
	SCM	32.51 (0.09)	31.83 (0.52)	30.30 (1.25)	30.61 (0.76)	32.24 (0.45)
Density σ_T (kg m^{-3})	Surface	25.11 (0.08)	24.82 (0.49)	19.20 (0.81)	22.95 (0.53)	25.39 (0.34)
	SCM	25.37 (0.11)	25.48 (0.42)	24.31 (1.04)	24.60 (0.62)	25.77 (0.28)
Stratification index (kg m^{-3})		1.01 (0.11)	1.49 (0.59)	6.83 (0.75)	2.08 (0.26)	1.42 (0.22)
chl a (µg L^{-1})	Surface	0.41 (0.10)	0.43 (0.22)	0.05 (0.01)	0.42 (0.23)	0.73 (0.15)
	SCM	0.48 (0.11)	1.44 (0.48)	0.18 (0.02)	0.69 (0.14)	1.03 (0.10)
NO$_3^-$ (µmol L^{-1})	Surface	8.74 (2.17)	4.07 (2.28)	0.27 (0.09)	0.93 (0.40)	1.25 (0.41)
	SCM	9.76 (2.27)	6.83 (2.55)	3.85 (1.35)	7.19 (1.52)	1.44 (0.38)
Si(OH)$_4$ (µmol L^{-1})	Surface	15.61 (2.49)	16.27 (3.26)	4.05 (0.89)	4.44 (0.95)	3.00 (0.86)
	SCM	19.59 (2.95)	25.61 (5.79)	12.44 (2.75)	14.10 (2.24)	3.65 (0.92)
PO$_4^{3-}$ (µmol L^{-1})	Surface	1.07 (0.12)	0.93 (0.26)	0.57 (0.06)	0.72 (0.13)	0.60 (0.18)
	SCM	1.27 (0.16)	1.61 (0.30)	1.14 (0.11)	0.77 (0.09)	0.35 (0.12)
NH$_4^+$ (µmol L^{-1})	Surface	0.52 (0.22)	0.50 (0.45)	0.05 (0.00)	0.08 (0.02)	0.14 (0.05)
	SCM	0.84 (0.26)	1.13 (0.47)	0.10 (0.05)	0.12 (0.03)	0.16 (0.07)
Urea (µmol N L^{-1})	Surface	0.46 (0.12)	0.88 (0.26)	0.65 (0.12)	0.47 (0.09)	0.56 (0.06)
	SCM	0.58 (0.19)	0.99 (0.26)	0.87 (0.16)	0.77 (0.21)	0.60 (0.07)
Dissolved inorganic carbon DIC (µmol L^{-1})	Surface	2046.1 (19.4)	1983.8 (43.1)	1748.6 (29.6)	1915.6 (13.6)	2015.2 (32.3)
	SCM	2057.6 (10.8)	2073.5 (46.0)	2045.0 (44.3)	2054.3 (38.7)	2042.8 (30.7)

DIC samples were analyzed and provided by the Institute of Ocean Sciences, Fisheries and Oceans Canada (see Varela et al., 2013).
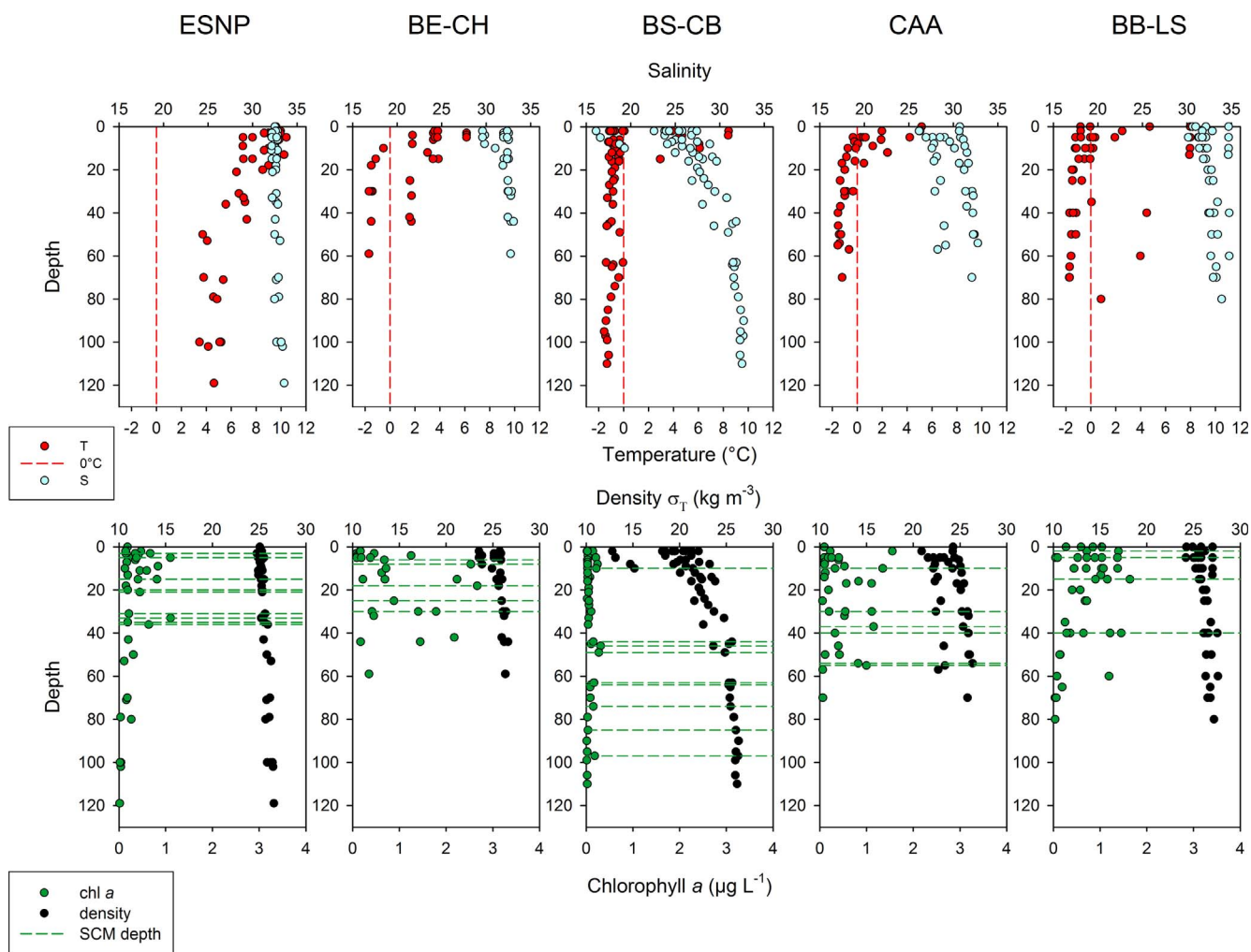
Fig. 2. Oceanographic profiles of salinity, temperature, density and chlorophyll *a* (chl *a*). Data source is Carmack and McLaughlin (2011) and Varela et al. (2013). Each panel represents a scatterplot of all sampling depths for all stations within each domain. Vertical dashed red lines represent 0 °C. Horizontal dashed green lines represent all the depths of the subsurface chlorophyll maximum (SCM) in each domain where samples were taken for phytoplankton taxonomical enumeration. (For interpretation of the references to colour in this figure legend, the reader is referred to the web version of this article.)

laboratory, 100 ml subsamples were settled for 48 h in sedimentation chambers (Utermöhl, 1958) and phytoplankton cells enumerated at 600× magnification with light microscopy (LM) using an Olympus IX-70 inverted microscope. Differentiation between autotrophic and heterotrophic cells was based upon the presence/absence of chloroplasts. We endeavored to count only autotrophic nano- and microphytoplankton, but given the limitations of LM we cannot guarantee that this was achieved in all cases. At least 300 individuals, all of them with full protoplasm, were counted in random fields, and cell abundances for each taxon were expressed as numbers of cells per litre of seawater. We classified phytoplankton groups based on the taxonomic Class level (-phyceae) to which they belong (as in Kubiszyn et al., 2017). Cells were identified to genus/species level, where possible, generally according to Tomas (1997) and Horner (2002). Since small naked mono- or biflagellated cells can be difficult to identify and many can lose their flagella after addition of fixatives, they were grouped together into two unidentified flagellate/coccoids categories (2–5 µm and 5–8 µm), which could therefore include a number of taxonomic groups. Total abundance of diatoms (Bacillariophyceae), dinoflagellates (Dinophyceae), cryptomonads (Cryptophyceae) and unidentified flagellates/coccoids (2–8 µm) were then calculated. When identifiable, abundances of species/genera for other taxonomic groups were also noted, such as prasinophyceans (Prasinophyceae), chlorophyceans (Chlorophyceae), euglenophyceans (Euglenophyceae), chrysophyceans

(Chrysophyceae) and silicoflagellates (Dictyochophyceae). Picophytoplankton (< 2 µm) such as *Synechococcus* were not generally counted although some picophytoplankton of around 2 µm may have been included in our counts when staining of the cells was irregular, denoting the presence of plastids. The diatom *Chaetoceros gelidus* can be easily misidentified as *Chaetoceros socialis*. Our identification was based upon a review of the recent literature concerning the morphological variation within the *C. socialis* complex (Degerlund et al., 2012; Gaonkar et al., 2017) and the distinguishing features of *C. gelidus* (Chamnansinp et al., 2013).

A scanning electron microscope (SEM) was also used for a more detailed examination and identification of certain taxa, principally diatoms. Samples were cleaned of organic matter according to the method of Hasle and Fryxell (1970), prepared on stubs and coated with gold-palladium according to Ferrario et al. (1995). SEM examination was conducted with a Hitachi S-3500N SEM in the Department of Biology at the University of Victoria, Canada.

2.4. Calculation of cellular biovolume and carbon biomass

Cell abundance and cell size were used to calculate total biovolume for all autotrophic cells > 2 µm by adopting the geometric shapes suggested by Hillebrand et al. (1999). Biovolume was then converted to total carbon biomass (C) for each taxon according to the C:volume
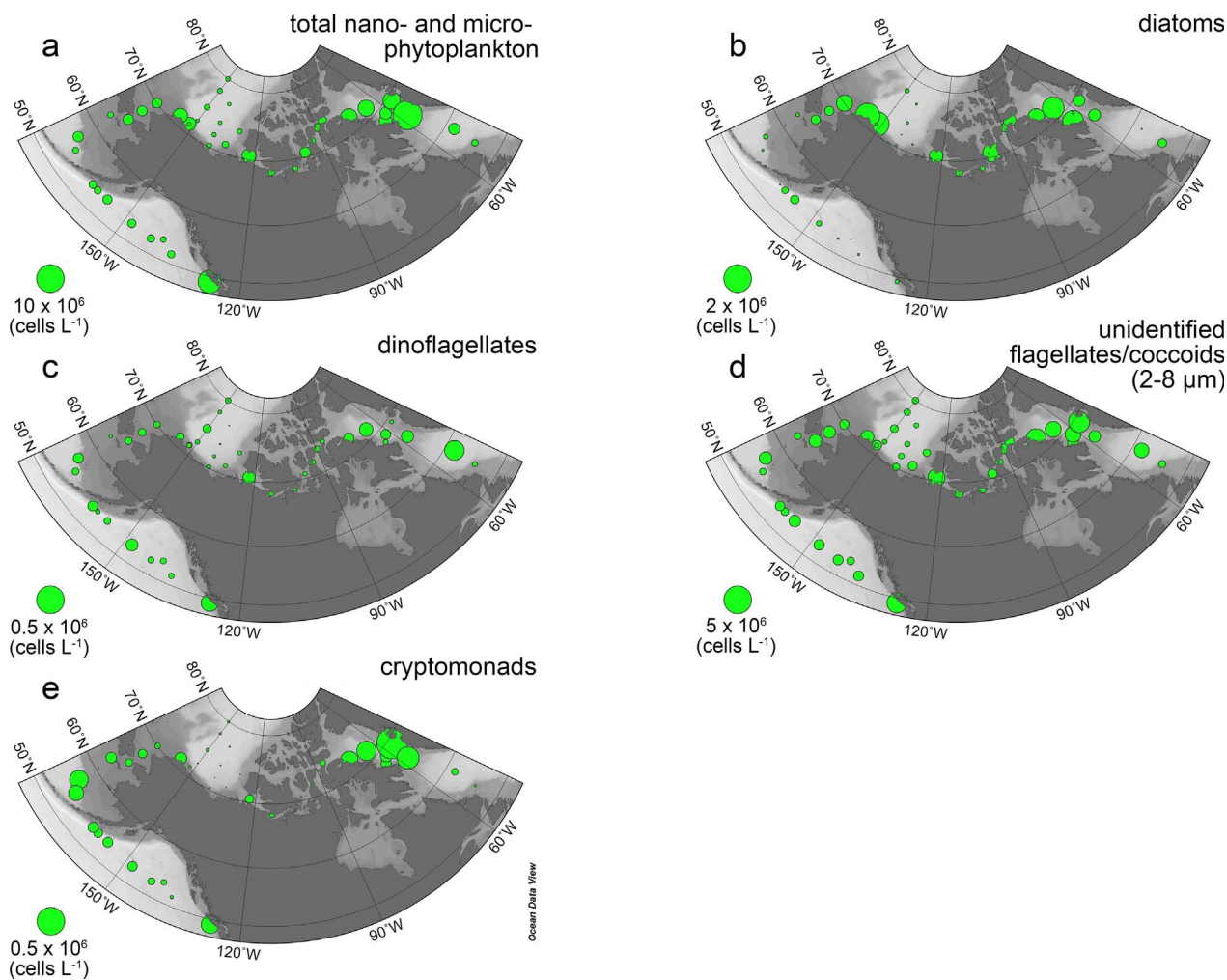
Fig. 3. Cell abundance of major groups of phytoplankton (> 2 μm) within the SCM across all full-profile stations in Subarctic and Arctic Seas, (a) total nano- and microphytoplankton, (b) diatoms (Bacillariophyceae) c) dinoflagellates (Dinophyceae), (d) unidentified flagellates/coccoids (2–8 μm), and (e) cryptomonads (Cryptophyceae). Abundance of each group is denoted at each station by the size of the coloured circles, with a reference circle shown to the left of each map. Note the variation in scale between panels.

(C:vol) equations of Menden-Deuer and Lessard (2000). The data presented throughout the paper is based upon separate equations for the C density (in pg μm^{-3}) of diatoms and of other non-diatom protists (Menden-Deuer and Lessard, 2000). However, in order to examine uncertainty of C estimates for selected representative taxa, we also estimated C biomass using the single C:vol equation for all protists proposed by Montagnes et al. (1994).

2.5. Ratios of phytoplankton carbon to chlorophyll a, and biogenic silica to phytoplankton carbon

Ratios of total phytoplankton C (> 2 μm) to chlorophyll *a* (phyto C:chl *a*), and biogenic silica (SiO$_2$ or bSi) to phytoplankton C (> 2 μm) (bSi:phyto C) were calculated at each station using the chl *a* and bSi data concurrently collected from the depth of the SCM (Varela et al., 2013; Wyatt et al., 2013).

3. Results

3.1. Oceanographic properties

The physical and chemical properties of the five domains in the C3O/JOIS programs, already described by Carmack and McLaughlin (2011) and Varela et al. (2013), are summarized here in Tables 1 and 2, and Fig. 2, together with the SCM depths where phytoplankton samples

were taken for the present study.

The subarctic domains ESNP and BB-LS were characterized by weak stratification of the water column (Table 2, Fig. 2). Based on the difference between the surface and the SCM depth, the upper water column was also relatively homogenous in concentrations of nitrate (NO$_3^-$), silicic acid (Si(OH)$_4$), orthophosphate (PO$_4^{3-}$), ammonium (NH$_4^+$) and urea-N (Table 2, see also Varela et al., 2013). Clearly, the BB-LS domain differed from the ESNP in having lower temperatures (Table 2, Fig. 2), and the presence of extensive ice cover at the Baffin Bay stations (Tables 1 and 2). Depths of the SCM were within the upper 40 m (Fig. 2, Tables 1 and 2), and always shallower than the average depth of 1% surface irradiance in both domains. The BE-CH domain was characterized by moderate ice cover at the northern stations (Table 1), and increasing density stratification as a result of lower surface temperature and salinity (Table 2, Fig. 2). Average depth of the SCM was < 20 m and at most stations shallower than the 1% surface irradiance depth (Table 2). Extensive ice cover, with low surface temperature and salinity, characterized the BS-CB and CAA domains (Tables 1 and 2, Fig. 2), leading to pronounced density stratification of the upper water column. However, the CAA differed from the BS-CB in having weaker stratification, and shallower average SCM depth and 1% surface irradiance depth.

Other than the stratification resulting from low salinity surface waters, particularly in the BS-CB and CAA, the most striking difference between domains was the gradient in nutrient concentrations between
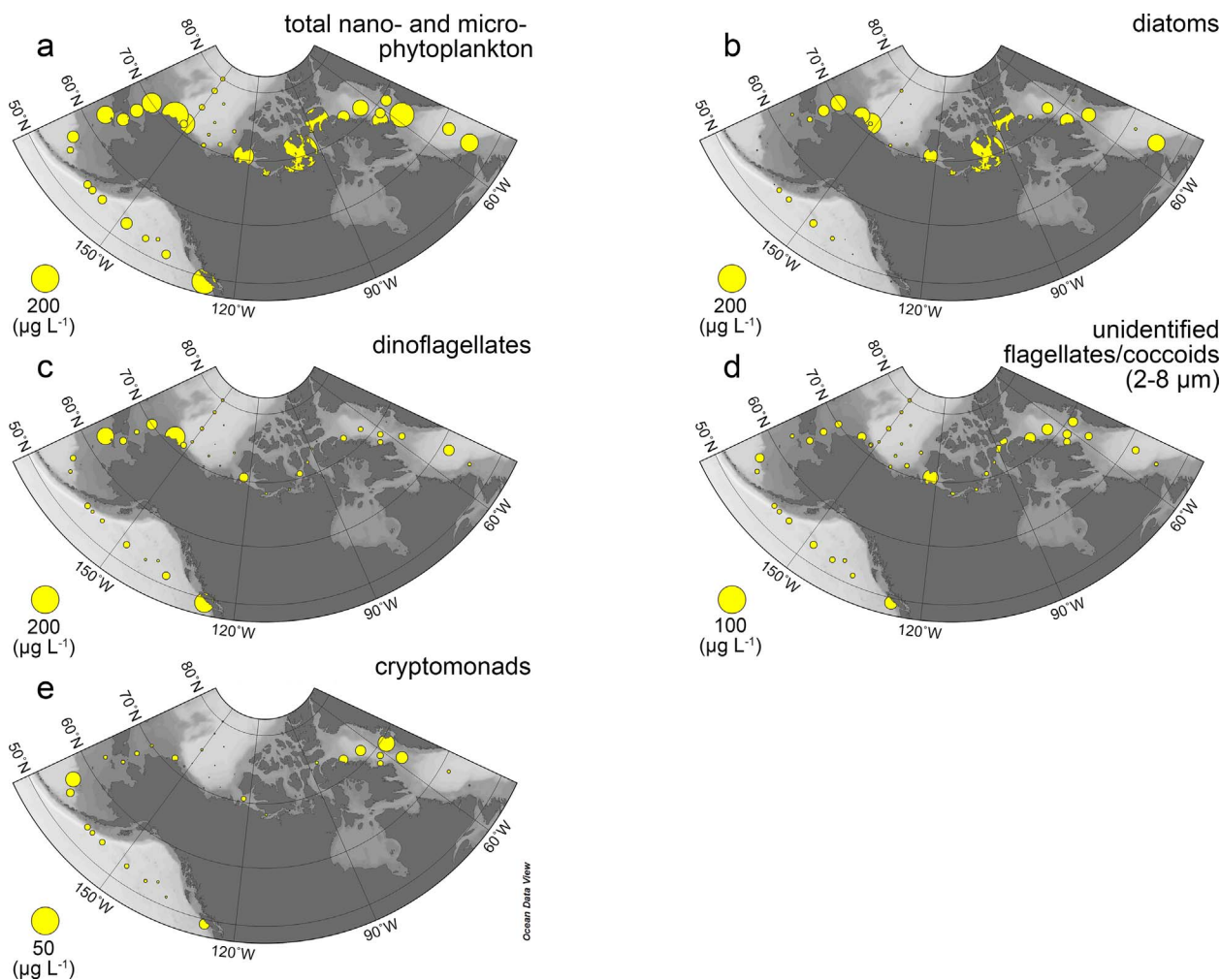
Fig. 4. Carbon biomass (C) of major groups of phytoplankton (> 2 µm) within the SCM across all full-profile stations in Subarctic and Arctic Seas, (a) total nano- and microphytoplankton, (b) diatoms (Bacillariophyceae), (c) dinoflagellates (Dinophyceae), (d) unidentified flagellates/coccoids (2–8 µm), and (e) cryptomonads (Cryptophyceae). Total C biomass for each group is denoted at each station by the size of the coloured circles, with a reference circle shown to the left of each map. Note the variation in scale between panels.

the ESNP in the west and the BB-LS in the east, particularly in terms of dissolved NO_3^- and $Si(OH)_4$ (Table 2). These nutrient and chl *a* concentrations and distributions are described in more detail by Varela et al. (2013).

3.2. Spatial variation in abundance and carbon biomass of nano- and microphytoplankton

Figs. 3 and 4 show abundance and carbon biomass (C) data for all stations where samples were taken from the SCM, including those omitted from domains (see Table 1). Total phytoplankton (> 2 µm) abundances reached 7.13×10^6 cells L^{-1} off the west coast of Vancouver Island at station NP-1, which is a coastal station omitted from the domains (see Table 1), and 11.2×10^6 cells L^{-1} in the Davis Strait, northern Labrador Sea, at station LS-7 (Fig. 3a). In contrast, the lowest total cell abundances of $\sim 0.19 \times 10^6$ cells L^{-1} occurred at stations CB-2a in the southwestern Canada Basin and CB-15 in the north-central Canada Basin (Fig. 3a). Large-scale variations in total cell abundance (Fig. 3a) were largely driven by variations in the abundance of unidentified flagellates/coccoids (2–8 µm) that reached a maximum of 2.94×10^6 cells L^{-1} at station BB-1 in Baffin Bay (Fig. 3d and Appendix). The highest abundance of autotrophic dinoflagellates of 0.26×10^6 cells L^{-1} occurred at station LS-4 in the Labrador Sea with minimum numbers of $< 0.001 \times 10^6$ cells L^{-1} at station CB-15 in the north-central Canada Basin (Fig. 3c and Appendix). Maximum diatom

numbers reached 1.60×10^6 cells L^{-1} at BL-2 (Fig. 3b and Appendix), a station located on the continental shelf east of the Chukchi Sea and excluded from both the BE-CH and BS-CB domains (Table 1). Higher diatom numbers (2.70×10^6 cells L^{-1}) were observed at surface station CB-28aa (data in Appendix only) located in the south Beaufort Sea. Cryptomonads exceeded $\sim 0.2 \times 10^6$ cells L^{-1} at station BS-5 in the southern Bering Sea and at several stations in the BB-LS domain, peaking at 0.63×10^6 cells L^{-1} at station BB-1 in eastern Baffin Bay off the coast of Greenland (Fig. 3e and Appendix).

Total phytoplankton cell C (> 2 µm) showed a similar distribution (Fig. 4a) to that of cell abundance (Fig. 3a), although unidentified flagellates/coccoids (2–8 µm) had little influence on the overall distribution pattern (Fig. 4a and d), which was largely driven by the C biomass of diatoms and autotrophic dinoflagellates (Fig. 4b and c). Dinoflagellate C reached $107.5 \, \mu g \, C \, L^{-1}$ at station BC-2 in the eastern Chukchi Sea off the coast of Alaska, and was $100.8 \, \mu g \, C \, L^{-1}$ at station NP-1 off Vancouver Island (Fig. 4c), where diatom C was only $0.41 \, \mu g \, C \, L^{-1}$ (Fig. 4b). Diatom C varied greatly, with the highest level for the entire study area of $331.6 \, \mu g \, C \, L^{-1}$ recorded at station CAA-10 in the Canadian Arctic Archipelago (Fig. 4b). Diatom C biomass levels of $< 0.1 \, \mu g \, C \, L^{-1}$ were measured at half of the offshore stations in the BS-CB domain, with no diatom C measured at the depth of the SCM at stations BI-2 in the eastern Canada Basin and CB-4 in the western Canada Basin (Fig. 4b). Cryptomonad C reached $15.4 \, \mu g \, C \, L^{-1}$ at station BS-5 in the southern Bering Sea, and $18.7 \, \mu g \, C \, L^{-1}$ at station BB-1 in eastern Baffin Bay (Fig. 4e).
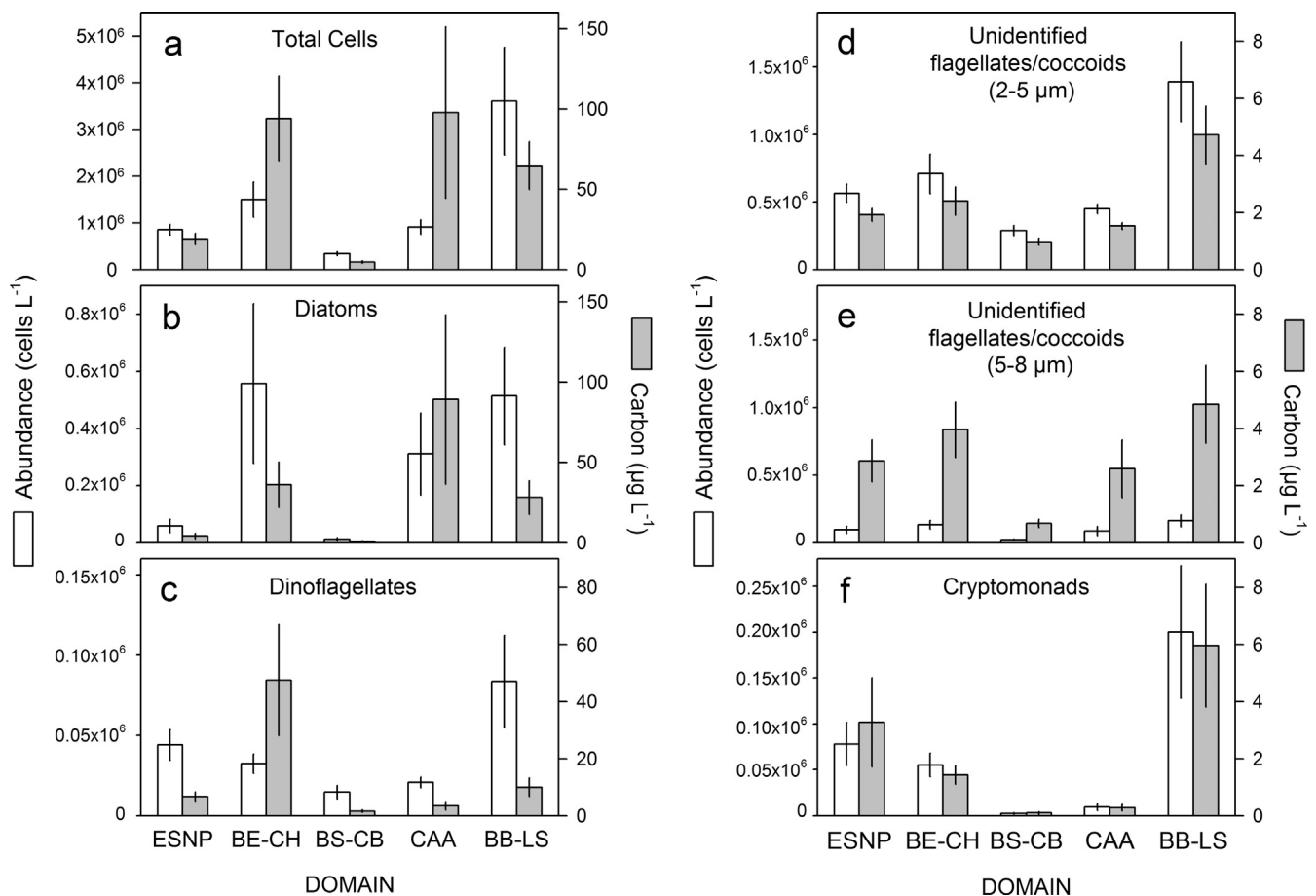
Fig. 5. Average cell abundance and carbon biomass (C) for major phytoplankton groups (> 2 μm) within the SCM in each oceanographic domain. Error bars denote ± one standard error (SE). (a) Total nano- and microphytoplankton, (b) diatoms (Bacillariophyceae), (c) dinoflagellates (Dinophyceae), (d) unidentified flagellates/coccoids (2–5 μm), (e) unidentified flagellates/coccoids (5–8 μm), and (f) cryptomonads (Cryptophyceae).

3.3. Domain averages of abundance and carbon biomass of nano- and microphytoplankton

Fig. 5 summarizes the average cell abundance and C biomass for the major phytoplankton groups. Average total cell abundance (Fig. 5a, Table 3) was highest ($3.61 \pm 1.15 \times 10^6$ cells L^{-1}) in BB-LS, lowest ($0.34 \pm 0.04 \times 10^6$ cells L^{-1}) in the BS-CB, and varied between 0.85 and 1.50×10^6 cells L^{-1} in the other three domains (ESNP, BE-CH and CAA). Average abundances of flagellates/coccoids (2–5 μm and 5–8 μm) (Fig. 5d and e) and dinoflagellates (Fig. 5c) were highest in the BB-LS. The high abundance of dinoflagellates observed at excluded station NP-1 (Fig. 3c and Appendix) did not contribute to the ESNP domain average (Fig. 5c). Average abundance of diatoms varied between 0.31×10^6 and 0.56 x10^6 cells L^{-1} in the BE-CH, CAA and BB-LS domains (Fig. 5b), with much lower numbers in the ESNP and BS-CB. Average abundance of cryptomonads was highest in the BB-LS domain (Fig. 5f), and was very low in the BS-CB and CAA.

Whereas variations in total phytoplankton (> 2 μm) abundance across domains (Fig. 5a, Table 3) were largely driven by the contribution of flagellates/coccoids (2–8 μm) (Fig. 5d, e, Table 3), variations in total phytoplankton C were dominated by the contribution of dinoflagellates and diatoms (Fig.5a, b and c, Table 3). Unidentified flagellates/coccoids (2–8 μm) averaged < 10 μg C L^{-1} in all domains, and < 5 μg C L^{-1} in ESNP, BS-CB and CAA (Fig.5d, e, Table 3). Total C biomass was highly variable between stations (Fig. 4), with the average (Fig. 5a) highest in the CAA (97.9 μg C L^{-1}) and slightly lower in the BE-CH (94.2 μg C L^{-1}) and BB-LS (64.9 μg C L^{-1}) domains (Table 3). Average total C biomass was 19.1 μg C L^{-1} in the ESNP and only 4.7 μg C L^{-1} in the BS-CB. Cryptomonads made a relatively small contribution

to overall biomass with average C of < 6 μg L^{-1} for all domains (Fig. 5f, Table 3).

Fig. 6 shows several 'minor' taxa that were identified in the samples but not included in Figs. 3–5. These taxa occurred in relatively low abundance with contributions to total C biomass that were largely insignificant. Except for *Phaeocystis* spp. (Fig. 6a) with a very high abundance at station LS-7 in the BB-LS, average C biomass for these groups did not exceed 1 μg L^{-1} for any other domain (Fig. 6 – note the variation in scales between panels). However, distributions of these taxa showed interesting trends. For example, the prasinophyceans *Pyramimonas* spp. occurred in much higher numbers in the BB-LS domain than in other domains (Fig. 6b), whereas the chrysophycean *Dinobryon balticum* (Fig. 6c) showed elevated abundance at some CAA stations. Abundances of silicoflagellates *Dictyocha speculum* were generally low, with domain averages < 1000 cells L^{-1}, and with a maximum average C biomass in the BS-CB domain (Fig. 6d). The abundance of euglenids, mainly *Eutreptiella* sp., showed no clear pattern (Fig. 6e), whereas the chlorophycean *Chlamydomonas* sp. was more abundant in the western domains, and less so in BS-CB (Fig. 6f).

3.4. Relative contribution of major taxonomic groups

The relative contribution of each taxonomic group to total cell abundance and C content was calculated for each station and then averaged by domain (Fig. 7 and Table 4). The 'others' group shown in Fig. 7 represented the sum of the minor taxa shown in Fig. 6. Unidentified flagellates/coccoids (2–8 μm) contributed on average 61–90% of total cell abundance over all domains (Fig. 7a, Table 4), but represented only 9–39% of total phytoplankton C (Fig. 7b, Table 4).
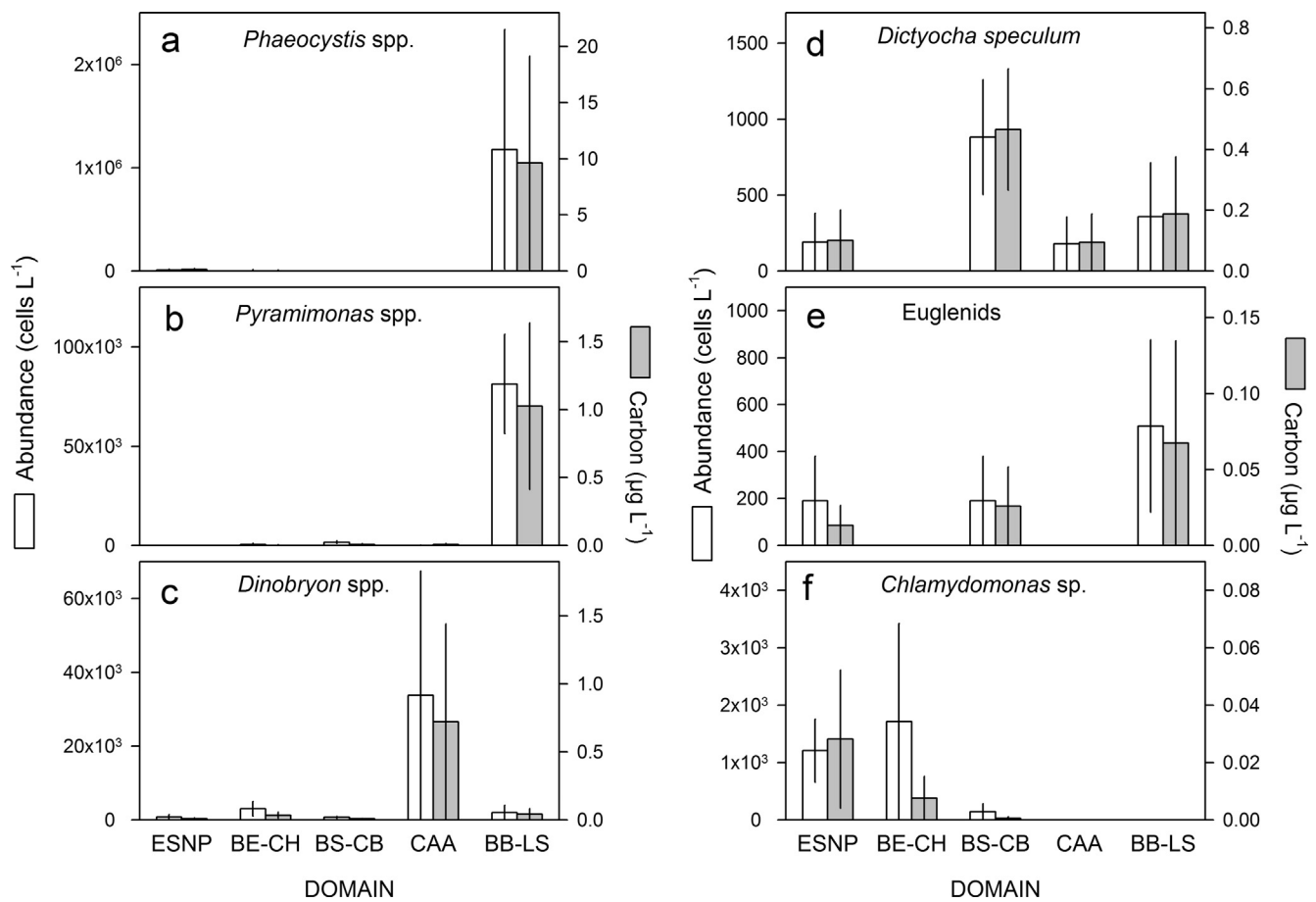
Fig. 6. Average cell abundance and carbon biomass (C) for several less common phytoplankton taxa within the SCM in each oceanographic domain. Error bars denote ± 1 SE. Note the variability in scales, since the abundance of these taxa span several orders of magnitude. These taxa were not included in the major groups shown in Fig. 5. (a) *Phaeocystis* spp. (Prymnesiophyceae), (b) *Pyramimonas* spp. (Prasinophyceae), (c) *Dinobryon* spp., mainly *Dinobryon balticum* (Chrysophyceae), (d) silicoflagellate *Dictyocha speculum* (Dictyochophyceae), (e) euglenids (Euglenophyceae, mainly *Eutreptiella* sp.) and (f) *Chlamydomonas* sp. (Chlorophyceae).

Despite relatively low abundances, dinoflagellates contributed significantly to total C biomass in the western domains (ESNP and BE-CH) and in the BS-CB. Diatoms averaged only 4–30% of total cell abundance (Fig. 7a, Table 4), but represented 18–70% of total phytoplankton C (> 2 μm) over the five domains (Fig. 7b, Table 4), with the greatest contribution to total C in the BE-CH, CAA and BB-LS domains. On average, the overall combined contribution of diatoms and dinoflagellates to total C biomass was ~55% in BB-LS and ESNP, > 80% in BE-CH and CAA, and ~49% in BS-CB. Flagellates/coccoids (2–8 μm) contributed 39% of total C biomass in the BS-CB, which was the highest relative contribution of the group for any domain.

Over the whole study area, there was a strong relationship, within the SCM, between total particulate organic carbon (POC) (Wyatt et al., 2013) and total phytoplankton C (> 2 μm) estimated from cell counts in the present study (Fig. 8a). Relationships were also evident between total POC in the SCM and the C biomass of diatoms (Fig. 8b), dinoflagellates (Fig. 8c) and unidentified flagellates/coccoids (2–8 μm) (Fig. 8d). In stations where POC in the SCM exceeded ~10 μmol C L^{-1}, diatoms and dinoflagellates made the dominant contribution to total C (Fig. 8b and c). However, where POC was ~1–10 μmol C L^{-1}, unidentified flagellates/coccoids (2–8 μm) made a greater relative contribution to total C (Fig. 8d).

3.5. Dominant taxa

Individual taxa can have significance either through consistent presence at many stations within a domain, or else, through a more sporadic occurrence, with high biomass at only a few stations within a

domain. The upper panel in Table 5 shows the average C biomass for the dominant phytoplankton taxa present at ≥ 50% of stations within each domain (50% is simply a nominal value chosen to highlight 'more common' taxa). The percentage of total stations in the domain at which each the taxa was present is also shown. The lower panel in Table 5 shows taxa present at < 50% of stations, but at biomass of > 1 μg C L^{-1} when averaged for the whole domain (here also, 1 μg C L^{-1} is simply a nominal average biomass chosen to highlight a 'significant' contribution). In other words, the lower panel of Table 5 highlights taxa typically present at elevated biomass but only at one or two stations within a domain. Some other taxa (e.g. those in Fig. 6) do not appear in Table 5 because of infrequent presence and/or average C biomass of < 1 μg L^{-1}.

Unidentified flagellates/coccoids (2–8 μm) and cryptomonads were almost ubiquitous through all domains, and because they could not be examined any further taxonomically, their total C contributions reported in Table 5 (upper panel) are the same as the domain averages shown in Fig. 5. Cryptomonads contributed more C in the BB-LS and ESNP domains (Fig. 5f and Table 5 upper panel), and showed a very low C biomass of only 0.09 μg C L^{-1} in the BS-CB.

Among the diatoms in the ESNP domain, only *Pseudo-nitzschia* spp. had a consistent presence (67% of stations), although at low biomass (Table 5 upper panel). The diatom *Neodenticula seminae* (Fig. 9a and b) was present in the ESNP but did not contribute significantly to C biomass (therefore does not feature in Table 5), and was not observed in other domains. *Corethron hystrix* was also noted sporadically in ESNP but not in other domains (Table 5 lower panel). *Gymnodinium* spp. (Table 5 upper panel) and *Tripos muelleri* (Fig. 9c, Table 5 lower panel)

a % ABUNDANCE **b** % CARBON

ESNP

BE-CH

BS-CB

CAA

BB-LS

- unidentified flagellates/coccoids (2-8 μm)
- dinoflagellates
- diatoms
- cryptomonads
- others
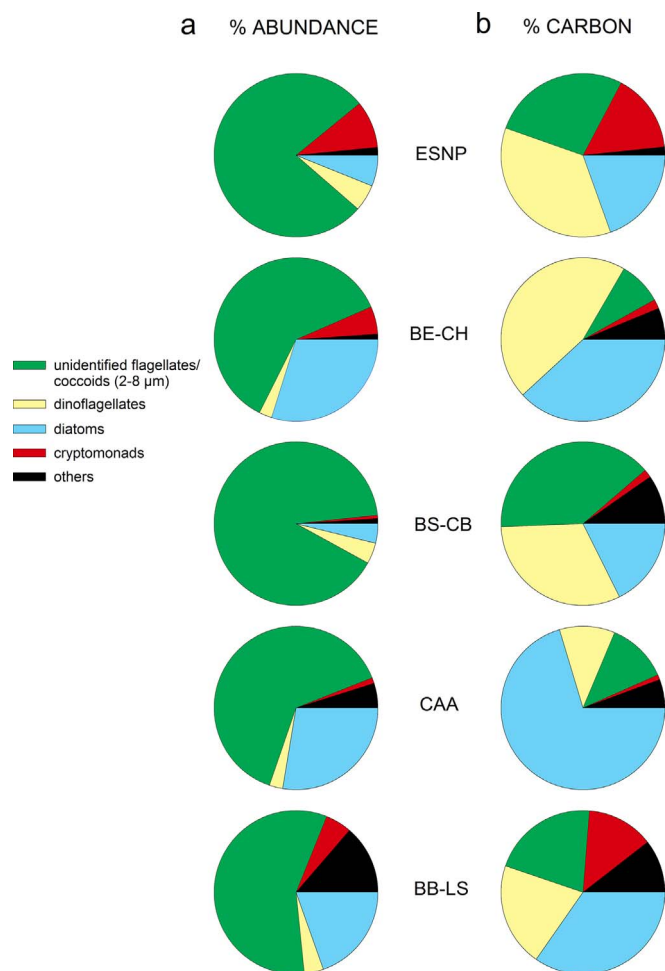
Fig. 7. Average percentage contribution of the major taxonomic groups to total abundance and carbon biomass (C) of phytoplankton (> 2 μm) within each oceanographic domain. Taxa not belonging to the four major groups are included in the 'others' category detailed in Fig. 6. Relative contributions were calculated for each station and then averaged for each domain. Data with standard errors are shown in Table 4.

were the only dinoflagellates that made significant contributions to C biomass in the ESNP.

The BE-CH domain was characterized by a rich diversity of diatoms. Some, such as *Chaetoceros gelidus* and *Cylindrotheca closterium,* were present at most stations (Table 5 upper panel). Other diatoms were

present at a single station (Table 5 lower panel), such as *Coscinodiscus wailesii* (Fig. 9d), and *Pauliella taeniata* (Fig. 9e and f). Several unidentified centric species were also notable (Table 5 upper panel). Of the dinoflagellates, *Gymnodinium* spp. and *Gyrodinium* spp. occurred at most stations (Table 5 upper panel), with *Alexandrium* sp. and *Peridiniella catenata* (Fig. 9 g) significant at individual stations (Table 5 lower panel).

Total phytoplankton C (> 2 μm) was very low in the BS-CB domain, with unidentified flagellates/coccoids (2–8 μm) and *Gymnodinium* spp. providing the most significant contributions (Table 5 upper panel). Although diatoms were present in low abundance (Figs. 3 and 5b) in BS-CB, no individual diatom species or genus made a noticeable contribution to total C biomass other than *Chaetoceros gelidus* (Table 5 upper panel, Fig. 9 h). However, diatoms contributed on average ~18% of total C in the BS-CB (Fig. 7, Table 4) suggesting that the bulk of this must have been contributed by species present at very low abundance (see Appendix). Prasinophyceans were present in the BS-CB domain, but did not contribute significantly to total phytoplankton C (Fig. 6). The chrysophycean *Dinobryon balticum* (Fig. 9i) was abundant at surface stations MK-3 and BL-4 in the BS-CB domain (see Appendix), but did not contribute significantly to total C biomass within the SCM (Fig. 6). The only phytoplankton taxon with average C higher in BS-CB than elsewhere was the silicoflagellate *Dictyocha speculum* (Fig. 9j), albeit with low C biomass (average < 0.5 μg C L^{-1}).

The CAA was characterized by high biomass of relatively few diatom taxa, principally *Thalassiosira* spp. (Fig. 9k, Table 5 upper panel) and particularly resting spores of *T. antarctica* var. *borealis* (Fig. 9l, m, Fig. 5 lower panel), together with other unidentified centric diatoms (Table 5 upper panel). Dinoflagellates were less significant in the CAA with only *Alexandrium* sp. (Table 5 lower panel) and *Gymnodinium* spp. (Table 5 upper panel) contributing an average of > 1 μg C L^{-1}. Average biomass of flagellates/coccoids (2–8 μm) in the CAA was lower than in the BE-CH domain (Table 5 upper panel).

Phytoplankton assemblages in the BB-LS domain (Table 5 upper panel) were dominated by flagellates/coccoids (2–8 μm), cryptomonads (Fig. 9n), *Gymnodinium* spp. (Fig. 9o, p), and various diatoms such as *Thalassiosira* spp., including, among others, *T. nordenskioeldii* (Fig. 9q, Table 5 lower panel) and *T. antarctica* var. *borealis* (Fig. 9r, Table 5 lower panel), *Chaetoceros gelidus* (Table 5 lower panel) and *Bacterosira bathyomphala* (Table 5 lower panel). Also present were pennate diatoms of the genus *Fragilariopsis* (Fig. 9s, Table 5 upper panel), the dinoflagellate *Pyrophacus* cf. *horologium* (Table 5 lower panel), and single cells of *Phaeocystis* spp. (prymnesiophycean, Table 5 lower panel). *Pyramimonas* spp. were also present at most stations, but with relatively low C biomass (Table 5 upper panel).

Table 3
Average abundance and carbon biomass (C) of total phytoplankton (> 2 μm), and each major taxonomic group in each oceanographic domain. Only data from the SCM for all full-profile stations were used. Standard error appears in parentheses. The 'others' group refer to the sum of the minor taxa shown in Fig. 6.

		ESNP	BE-CH	BS-CB	CAA	BB-LS
Average abundance (×10^6 cells L^{-1})	Total nano- and microphytoplankton	0.854 (0.108)	1.504 (0.380)	0.344 (0.042)	0.911 (0.156)	3.614 (1.152)
	Diatoms	0.058 (0.023)	0.558 (0.280)	0.012 (0.005)	0.311 (0.144)	0.514 (0.171)
	Dinoflagellates	0.044 (0.010)	0.036 (0.007)	0.015 (0.004)	0.021 (0.004)	0.088 (0.030)
	Unidentified flagellates/coccoids (2–5 μm)	0.565 (0.068)	0.708 (0.146)	0.289 (0.037)	0.449 (0.036)	1.390 (0.298)
	Unidentified flagellates/coccoids (5–8 μm)	0.096 (0.025)	0.132 (0.033)	0.023 (0.005)	0.086 (0.034)	0.162 (0.046)
	Cryptomonads	0.078 (0.023)	0.055 (0.013)	0.002 (0.001)	0.009 (0.004)	0.200 (0.072)
	Others	0.012 (0.006)	0.014 (0.006)	0.004 (0.001)	0.034 (0.034)	1.261 (1.164)
Average C (μg L^{-1})	Total nano- and microphytoplankton	19.13 (3.50)	94.16 (26.55)	4.70 (0.83)	97.89 (53.54)	64.92 (14.89)
	Diatoms	4.09 (1.76)	36.19 (14.25)	0.86 (0.38)	89.22 (52.83)	28.25 (10.62)
	Dinoflagellates	6.71 (1.61)	47.51 (19.46)	1.59 (0.42)	3.46 (1.50)	9.96 (3.28)
	Unidentified flagellates/coccoids (2–5 μm)	1.92 (0.23)	2.40 (0.50)	0.98 (0.13)	1.53 (0.12)	4.72 (1.01)
	Unidentified flagellates/coccoids (5–8 μm)	2.87 (0.74)	3.96 (0.98)	0.68 (0.14)	2.59 (1.01)	4.85 (1.37)
	Cryptomonads	3.27 (1.56)	1.42 (0.33)	0.09 (0.04)	0.28 (0.12)	5.96 (2.16)
	Others	0.27 (0.15)	2.67 (2.55)	0.51 (0.20)	0.82 (0.71)	11.18 (9.39)

Table 4

Average percentage contribution of the major taxonomic groups to total abundance and carbon biomass (C) of phytoplankton (> 2 μm) in each oceanographic domain. Only data from the SCM for all full-profile stations were used. The % abundance or % C biomass for each group was calculated for each station within each domain, and then averaged for the domain in question; this calculation allows presentation of the standard error for each group (in parentheses). Data also appears graphically in Fig. 7. The 'others' group refer to the sum of the minor taxa shown in Fig. 6.

		ESNP	BE-CH	BS-CB	CAA	BB-LS
Average % Total Phytoplankton Abundance	Diatoms	6.12 (2.30)	29.80 (9.83)	3.88 (1.55)	27.60 (8.33)	19.57 (6.81)
	Dinoflagellates	5.28 (0.94)	2.55 (0.27)	4.12 (1.02)	2.65 (0.59)	3.79 (1.74)
	Unidentified flagellates/coccoids (2–8 μm)	77.71 (3.82)	61.13 (8.16)	90.34 (1.52)	63.76 (6.47)	57.76 (8.83)
	Cryptomonads	9.35 (2.82)	5.46 (2.77)	0.67 (0.20)	1.13 (0.41)	5.21 (1.64)
	Others	1.54 (0.90)	1.06 (0.45)	0.99 (0.28)	4.86 (4.83)	13.67 (10.13)
Average % Total Phytoplankton C	Diatoms	19.52 (7.00)	38.13 (12.69)	17.63 (6.77)	70.39 (14.23)	34.65 (12.37)
	Dinoflagellates	35.88 (6.72)	45.27 (13.74)	31.75 (6.21)	10.96 (6.51)	20.56 (8.38)
	Unidentified flagellates/coccoids (2–8 μm)	27.33 (3.13)	8.54 (2.40)	39.32 (4.07)	12.04 (4.06)	21.04 (5.27)
	Cryptomonads	15.65 (4.81)	1.84 (0.46)	1.65 (0.52)	0.99 (0.49)	13.25 (6.65)
	Others	1.63 (0.96)	6.23 (6.01)	9.64 (3.29)	5.63 (5.01)	10.49 (6.00)

3.6. Ratios of phytoplankton carbon to chlorophyll a, and biogenic silica to phytoplankton carbon

Using the taxonomic analysis of the phytoplankton assemblage presented here, and the concentrations of biogenic particles for the same stations (from Varela et al., 2013; Wyatt et al., 2013), we calculated ratios of phytoplankton C to chl *a* (phyto C:chl *a*), and biogenic silica to phytoplankton C (bSi:phyto C). Domain averages for phyto C:chl *a* were in the range 51 to 87 g C g chl *a*$^{-1}$ in the ESNP, BB-LS and BE-CH domains, but only 31 g C g chl *a*$^{-1}$ in the BS-CB (Fig. 10a). In the CAA, the high average phyto C:chl *a* ratio (150 ± 76 g C g chl *a*$^{-1}$) was substantially skewed by stations CAA-2 and CAA-10, where very high levels of phytoplankton C were not accompanied by significant increases in chl *a*. These two stations coincided with elevated abundance of diatom resting spores, conceivably with higher C:chl *a* ratios than in vegetative cells. Ratios of bSi:phyto C decreased from an average of 0.49 (± 0.19) mol Si mol C^{-1} in the BE-CH domain, to 0.22 (± 0.09) mol Si mol C^{-1} in the BB-LS domain (Fig. 10b).

4. Discussion

### 4.1. Approach and strengths of this study

The present study maximized regional coverage, minimized the role of seasonal variability by sampling only in summer (July–August), and maintained consistency in methodology and taxonomic definitions throughout all regions. However, some limitations to this approach remain. Firstly, in order to maximize regional coverage whilst at the same time maintaining the logistics of sample processing to a realistic level, only samples from the depth of the SCM were processed, as in several other studies (e.g. Ardyna et al., 2011). Although phytoplankton within the SCM make a large contribution to total water column production in Arctic waters (Martin et al., 2012), it is unclear to what extent these assemblages within the SCM are representative of the water column. Reasonable agreement between SCM and surface samples has been documented, at least for some taxa (Booth, 1988; Joo et al., 2012), although in the Beaufort Sea in summer, Balzano et al. (2012) have reported increased numbers of nanophytoplankton in the SCM compared to the surface. The SCM can also at times include sea-ice unicellular autotrophs, as well as phytoplankton, and species such as *Nitzschia frigida* were sporadically observed in the present study. Secondly, with such high variability of physical, chemical and biological properties over such a wide geographical area, potential temporal effects on our data cannot be fully separated from spatial variability, as noted by Varela et al. (2013). Finally, light microscopy provides limited taxonomic information on smaller phytoplankton (Booth, 1987) and preservatives may have differential effects on taxonomic groups (Booth, 1988). Therefore, some heterotrophic protists may have been included in our "unidentified flagellate/coccoid (2–8 μm)" fraction.

Robust comparisons between studies, both at a pan-Arctic scale and at the smaller scale, have been hampered by methodological inconsistencies. Definitions and categories for cell size, trophic status and taxonomic classification often differ between studies, and data for individual taxa have been reported in terms of cell abundance (Booth, 1988; Booth et al., 1993; Booth and Horner, 1997; Schloss et al., 2008; Sukhanova et al., 2009; Ardyna et al., 2011; Joo et al., 2012), total biovolume (e.g. Joo et al., 2012), or total C biomass (Booth, 1988; Booth et al., 1993; Booth and Horner, 1997; Gosselin et al., 1997; Sukhanova et al., 2009). This variety of approaches has further complicated between-study comparisons of C contributions by various taxa. The present study has attempted to minimize these inconsistencies and provides comparative estimates of abundance and biomass across a wide geographical area.

4.2. Oceanographic features of the domains

To facilitate interpretation of taxonomic data, we provide here a summary of the physical, chemical and biological features of the five domains, originally more fully described by Carmack and McLaughlin (2011) and later by Varela et al. (2013).

In the ESNP domain, temperature, salinity and density at the surface and within the SCM indicated relatively low stratification within the euphotic zone, with low concentrations of chl *a* and high concentrations of NO$_3^-$ consistent with phytoplankton constrained by the availability of iron over much of this domain (e.g. Boyd et al., 1996; Boyd et al., 2004). Water column stratification was also relatively weak in the BE-CH, although stronger than in the ESNP. A pronounced SCM and notable drawdown in surface NO$_3^-$ concentrations were evident in the BE-CH during the July study period, consistent with a domain strongly influenced by seasonal cycles, early sea-ice melt, and enriched by nutrient-laden Pacific water earlier in the season (e.g. Walsh et al., 1989; Carmack and McLaughlin, 2011). The BS-CB domain was characterized by extensive ice-cover, low salinity surface waters, and a deep euphotic zone. Average summer surface concentrations of NO$_3^-$ of 0.27 μmol L^{-1} and chl *a* of 0.05 μg L^{-1} were consistent with previous observations of a highly stratified oligotrophic system with a deep SCM and phytoplankton limited principally by irradiance and the vertical supply of NO$_3^-$ (Carmack and McLaughlin, 2011). Although weaker than in the BS-CB, stratification was also evident in the vertical distributions of density and NO$_3^-$ in the CAA. Surface NO$_3^-$ and chl *a* were higher in the CAA than in the BS-CB, and SCM layers were shallower, possibly as a result of mixing processes that enrich surface waters and favor phytoplankton growth in this topographically complex domain (Carmack and McLaughlin, 2011). The upper water column of the BB-LS was characterized by weaker density stratification than in the CAA, with relatively high chl *a* concentrations in both surface waters and the SCM. Compared to the western domains, summer concentrations of NO$_3^-$ and Si(OH)$_4$ in the BB-LS were low in both surface waters and within the SCM (Varela et al., 2013).
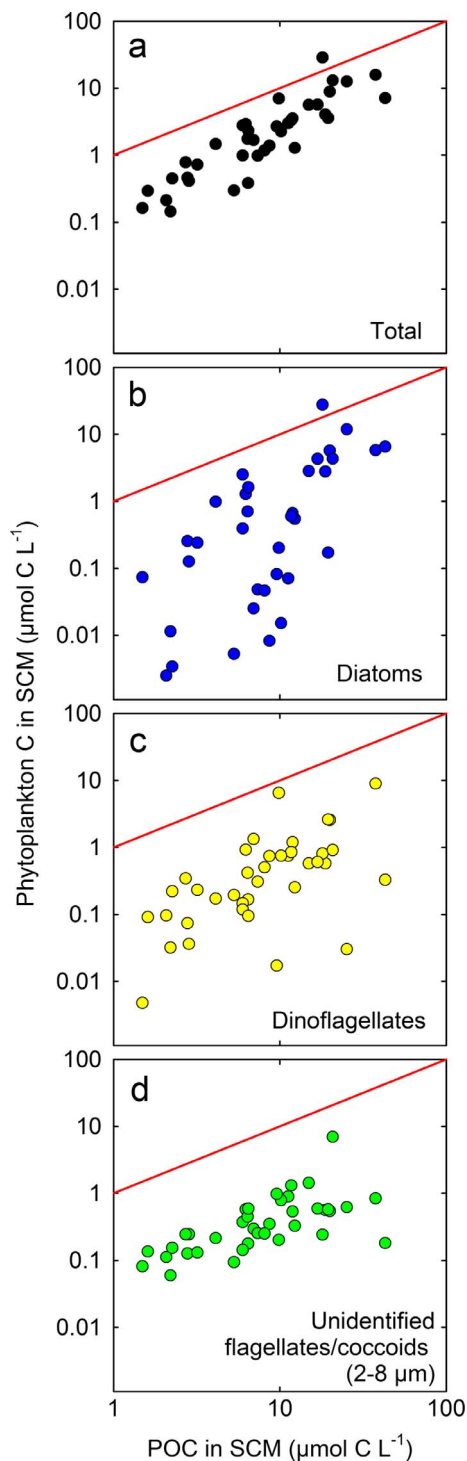
Fig. 8. Relationship between total particulate organic carbon (POC) at the depth of the SCM (from Wyatt et al., 2013) and carbon biomass (C) for the major phytoplankton taxa (> 2 μm) sampled from within the SCM during the present study. (a) Total nano- and microphytoplankton C, (b) diatom C, (c) dinoflagellate C and (d) unidentified flagellates/coccoids C (2–8 μm; sum of 2–5 μm and 5–8 μm fractions). Solid red lines represent 1:1 relationship between POC and total phytoplankton C (> 2 μm). (For interpretation of the references to colour in this figure legend, the reader is referred to the web version of this article.)

4.3. Comparison of phytoplankton assemblages with previous studies

The most extensive study of phytoplankton assemblages in the open ocean ESNP to date (Booth, 1988) noted vertical variability in total phytoplankton C and ta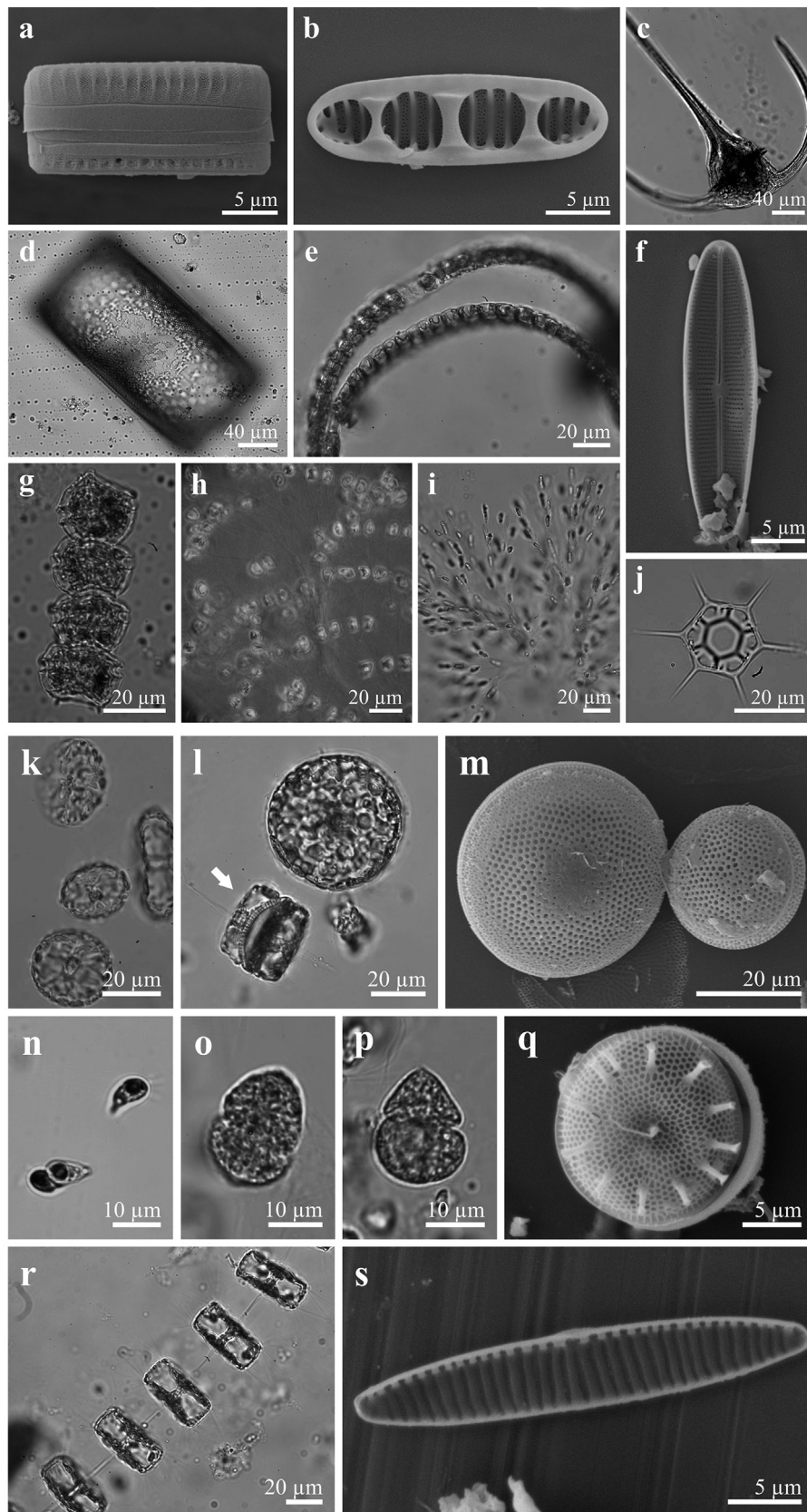xonomic composition throughout the euphotic zone in August 1984 at Ocean Station Papa (OSP, 50°N 145°W). The numerical dominance by unidentified 2–8 μm flagellates/coccoids (78% of total abundance, on average) in our study was in good agreement with that of Booth (1988) where small cells (< 5 μm) were shown to represent 67% of total abundance. These unidentified flagellates/coccoids averaged 4.8 μg C L^{-1} of the 19.1 ± 3.5 μg C L^{-1} for total nano- and microphytoplankton C in our study, compared to ~4 μg C L^{-1} in the < 5 μm fraction of the total C of ~8–12 μg C L^{-1} (estimated from the graphs of Booth, 1988). Diatoms represented on average 4.1 ± 1.8 μg C L^{-1} in the present study, compared to < 1 to 9 μg C L^{-1} in Booth (1988). Booth et al. (1993) extended the 1984 study of Booth (1988) to include data from the summer of 1988 and reported an average of 20 μg C L^{-1} for total phytoplankton C in the upper 60 m at OSP, with large diatoms (> 24 μm) contributing an average of ~7 to 8 μg C L^{-1} (Booth et al., 1993). The dominance of total C biomass by unidentified flagellates/coccoids (2–8 μm) in the ESNP is consistent with studies showing that the bulk of new production and nitrate uptake occurs in the < 5 μm fraction (Varela et al., 2013). With relatively low concentrations of bSi, and with ~80% total chl *a* in the < 5 μm fraction (Wyatt et al., 2013), our observations are consistent with an open ocean system numerically dominated by small phytoplankton (Varela and Harrison, 1999; Harrison, 2002; Peña and Varela, 2007), and with growth of large diatoms limited by iron availability (Boyd et al., 1996; Boyd et al., 2004).

Total phytoplankton C of 264 and 424 μg C L^{-1} was measured in the SCM at two stations in summer 1994 in the Chukchi Sea (Booth and Horner, 1997), and 285 μg C L^{-1} at 36 m depth on the Chukchi Shelf in summer 2002 (Sukhanova et al., 2009). The domain average in the present study of 94.2 ± 26.6 μg C L^{-1} was lower but consistent with that of ~100 μg C L^{-1} for late summer 2008 on the Chukchi Shelf (Coupel et al., 2012). Our measurements of C biomass for unidentified flagellates/coccoids (2–8 μm) of 2.4–10.1 μg C L^{-1} in the BE-CH were similar to those of 1.8 and 6.3 μg C L^{-1} for the 2–10 μm 'flagellate' fraction for two stations in the Chukchi Sea (Booth and Horner, 1997). These ranges were much lower however than the highly variable nanophytoplankton fraction (34.3 ± 34.2 μg C L^{-1}) for the Chukchi Shelf in late summer 2008 (Coupel et al., 2012), and the 4–10 μm flagellate fraction (0.6–159 μg C L^{-1}) reported by Sukhanova et al. (2009) for similar depths in the Bering Strait and the Chukchi Shelf in summer 2002. Total nano- and microphytoplankton C in the BE-CH was ~5-fold higher than in the ESNP in the present study, with the unidentified flagellate/coccoid fraction (2–8 μm) only ~30% higher than in the ESNP. The elevated total C in the BE-CH was therefore principally driven by larger cells, with diatoms representing ~38% and dinoflagellates ~45% of total C. Diatom C averaging 36.2 ± 14.3 μg C L^{-1} for the BE-CH in our study was in reasonable agreement with the 55.8 μg C L^{-1} for diatoms on the Chukchi shelf during late summer 2008 (Coupel et al., 2012). However, average diatom C biomass was lower than the maximum of 125 μg C L^{-1} on the Chukchi Shelf in summer 2002 (Sukhanova et al., 2009), and two measurements of ~410 and ~260 μg C L^{-1} on the central Chukchi Shelf in 1994 (Booth and Horner, 1997). Dinoflagellate C measurements on the Chukchi Shelf of 4.2 and 1.3 μg C L^{-1} (Booth and Horner, 1997), and < 1 μg C L^{-1} (Sukhanova et al., 2009) were much lower than our domain average of 47.5 (± 19.5 μg C L^{-1}) and that of 10.2 μg C L^{-1} for the summer of 2008 (Coupel et al., 2012). The abundance range of 0.007–0.037 × 10^6 cells L^{-1} for the dominant dinoflagellates *Gymnodinium* spp. was a little lower in our study than that of 0.012–0.100 × 10^6 for an unidentified *Gymnodinium* sp. in the Chukchi Sea in summer 2008 reported by Joo et al. (2012), who also corroborated our observation of elevated abundance of cryptomonads in the south Bering Sea. Our abundance measurements for *Chaetoceros* spp., *Thalassiosira* spp. and *Fragilariopsis* spp. in the BE-CH were also of a similar order to those reported for the SCM by Joo et al. (2012). Domination of total C by large cells (e.g. *Gymnodinium*, *Thalassiosira*, *Coscinodiscus*, and unidentified centric diatoms) in the BE-CH is

Table 5

Upper Panel: Average carbon biomass (C) for phytoplankton taxa present at ≥50% of stations in each of the Arctic and Subarctic domains. For each domain, the column to the right indicates the percentage of stations in a domain (% St) in which the taxa was present.

Group	Taxa present at ≥50% of stations within each domain	ESNP μg C L⁻¹ (± SE)	ESNP % St	BE-CH μg C L⁻¹ (± SE)	BE-CH % St	BS-CB μg C L⁻¹ (± SE)	BS-CB % St	CAA μg C L⁻¹ (± SE)	CAA % St	BB-LS μg C L⁻¹ (± SE)	BB-LS % St
						DOMAIN					
Unidentified flagellates/coccoids (2–8 μm)	Unidentified flagellates/coccoids 2–5 μm	1.92 (0.23)	100	2.40 (0.50)	100	0.98 (0.13)	100	1.53 (0.12)	100	4.72 (1.01)	100
	Unidentified flagellates/coccoids 5–8 μm	2.87 (0.74)	100	3.96 (0.98)	100	0.68 (0.14)	100	2.59 (1.01)	100	4.85 (1.37)	100
Dinoflagellates (Dinophyceae)	*Amphidinium* spp.	3.90 (1.03)	100	36.60 (17.36)	100	1.09 (0.31)	90	0.55 (0.36)	50	5.52 (1.28)	100
	Gymnodinium spp.	0.67 (0.30)	56	2.42 (1.52)	56			1.28 (0.53)	100		
	Gyrodinium spp.										
Cryptomonads (Cryptophyceae)	*Plagioselmis* cf. *prolonga*										
	Unidentified cells	3.27 (1.56)	100	1.42 (0.33)	100	0.09 (0.04)	70	0.28 (0.12)	83	4.90 (2.30)	63
Prasinophyceae	*Pyramimonas* spp.									0.37 (0.15)	88
Chrysophyceae	*Dinobryon balticum* (Schütt) Lemmermann			0.03 (0.02)	60						
Diatoms (Bacillariophyceae)	*Chaetoceros gelidus* Chamnansinp, Li, Lundholm & Moestrup			6.71 (3.69)	100	0.10 (0.06)	50	1.10 (0.30)	100	0.94 (0.61)	50
	Chaetoceros spp.			0.21 (0.08)	80					0.56 (0.26)	50
	Cylindrotheca closterium (Ehrenberg) Reimann & Lewin									0.33 (0.21)	50
	Fragilariopsis cylindrus (Grunow ex Cleve) Frenguelli							0.01 (0.00)	50		
	Fragilariopsis nana (Steemann Nielsen) Paasche							0.08 (0.07)	50	0.04 (0.02)	63
	Pseudo-nitzschia spp.	0.22 (0.10)	67					59.04 (50.19)	67		
	Thalassiosira spp.			6.01 (2.70)	80			10.40 (4.15)	83	9.90 (5.92)	50
	Unidentified centric diatoms > 15 μm							0.08 (0.05)	67		
	Unidentified centric diatoms < 15 μm										
Silicoflagellates (Dictyochophyceae)	*Dictyocha speculum* Ehrenberg					0.47 (0.20)	50				
Total C from taxa in upper panel		12.85		59.76		3.41		76.92		32.14	

144

Lower Panel: Average carbon biomass (C) for phytoplankton taxa present at < 50% of stations in each of the Arctic and Subarctic domains, but with a domain average of > 1 μg C L⁻¹ (a nominal figure chosen to represent a 'significant' average biomass). These species/genera occur more sporadically than the taxa shown in the upper panel, but can represent high levels of C at certain stations. Note that some taxa can appear in certain domains in the upper panel of the table, but in other domains in the lower panel.

| | DOMAIN | | | | | | | | | |
| | ESNP | | BE-CH | | BS-CB | | CAA | | BB-LS | |
Taxa present at < 50% of stations within each domain but with a domain average of > 1 μg C L⁻¹	μg C L⁻¹ (±SE)	% St	μg C L⁻¹ (±SE)	% St	μg C L⁻¹ (±SE)	% St	μg C L⁻¹ (±SE)	% St	μg C L⁻¹ (±SE)	% St
Dinoflagellates (Dinophyceae)										
Alexandrium sp.			1.89 (1.20)	40			1.62 (1.45)	33		
Peridiniella catenata (Levander) Balech			2.00 (2.00)	20					2.25 (1.59)	25
Pyrophacus horologium Stein										
Tripos muelleri Bory	1.59 (1.59)	11								
Unidentified cells			4.34 (4.34)	20						
Diatoms (Bacillariophyceae)										
Bacterosira bathyomphala (Cleve) Syvertsen & Hasle									1.54 (1.54)	13
Chaetoceros gelidus Chamnansinp, Li, Lundholm & Moestrup	1.20 (0.81)	22							2.21 (1.58)	43
Corethron hystrix Hensen										
Coscinodiscus sp.							1.90 (1.90)	17		
Coscinodiscus wailesii Gran & Angst			3.81 (3.81)	20						
Nitzschia frigida Grunow			1.15 (1.15)	20						
Pauliella taeniata (Grunow) Round & Basson			5.27 (5.27)	20						
Thalassiosira antarctica var. borealis Fryxell, Doucette & Hubbard									5.35 (5.35)	13
Thalassiosira antarctica var. borealis Fryxell, Doucette & Hubbard resting spores							11.58 (11.58)	17		
Thalassiosira sp. in resting spores			1.16 (1.16)	20						
Thalassiosira nordenskioeldii Cleve									1.91 (1.26)	25
Thalassiosira spp.			8.57 (8.57)	20						
Unidentified centric diatoms > 15 μm									1.59 (1.43)	25
Unidentified centric diatoms < 15 μm									2.28 (2.22)	38
Prymnesiophyceae										
Phaeocystis spp. (single cells)									9.52 (9.52)	13
Raphidophyceae										
Heterosigma sp.			2.55 (2.55)	20						
Total C from taxa in lower panel	2.79		30.73		0.00		15.11		26.66	
Average total phytoplankton C [a]	19.13		94.16		4.70		97.89		64.92	

[a] Average total phytoplankton C for each domain is higher than the sum of the totals in upper and lowers panels, because of less abundant taxa not shown here. The dominant taxa shown in the two panels typically account for > 70% of the average total phytoplankton C biomass for each domain.

Fig. 9. Light micrographs (LM) and scanning electron micrographs (SEM) of selected phytoplankton taxa observed across Subarctic and Arctic Seas around northern North America. Scale bars are given on each micrograph. (a) Diatom *Neodenticula seminae* (SEM). Frustule in girdle view. (b) Diatom *Neodenticula seminae* (SEM). Valve in internal view. (c) Dinoflagellate *Tripos muelleri* (LM). d) Diatom *Coscinodiscus wailesii* (LM). Cell in girdle view. (e) Diatom *Pauliella taeniata* (LM). Cells in ribbon-shaped colonies in apical view. (f) Diatom *Pauliella taeniata* (SEM). Valve with raphe in internal view. (g) Dinoflagellate *Peridiniella catenata* (LM). Cells in a colony. (h) Diatom *Chaetoceros gelidus* (LM). Cells forming spherical colonies. (i) Chrysophycean *Dinobryon balticum* (LM). Cells in loricae forming branched colonies. (j) Silicoflagellate *Dictyocha speculum* (LM). Silica skeleton. (k) Cells of diatom *Thalassiosira* spp. (LM). (l) Single cell of a centric diatom, and resting spore of *Thalassiosira antarctica* var. *borealis* indicated with arrow (LM). (m) Resting spores of the diatom *T. antarctica* var. *borealis* (SEM). (n) Cryptomonad cells (LM). (o) and (p) Dinoflagellate *Gymnodinium* spp. (LM). (q) Diatom *Thalassiosira nordenskioeldii* (SEM). (r) Diatom *T. antarctica* var. *borealis* (LM). Cells in long chain. (s) Diatom *Fragilariopsis oceanica* (SEM). Valve in internal view.

consistent with studies showing that the > 5 μm size fraction contributes > 60% of new production, nitrate uptake, and total chl *a* (Varela et al., 2013, Wyatt et al., 2013), and with bSi > 4-fold higher than in the ESNP (Wyatt et al., 2013).

In the BS-CB domain, the phytoplankton assemblage was numerically dominated (~90%) by unidentified flagellates/coccoids (2–8 μm), with average abundance falling within the range observed for nanophytoplankton by Balzano et al. (2012) within the SCM of the deeper
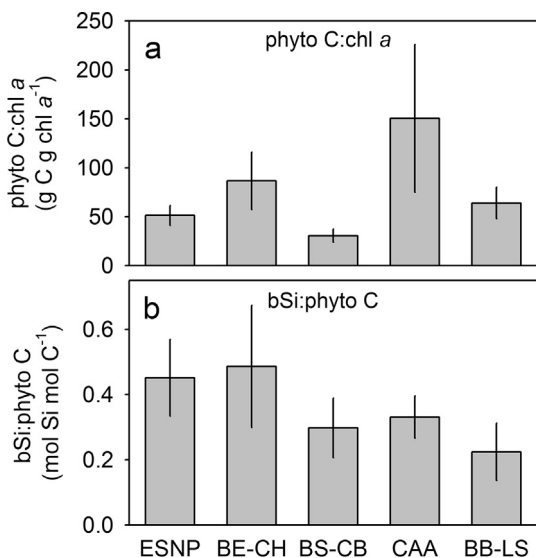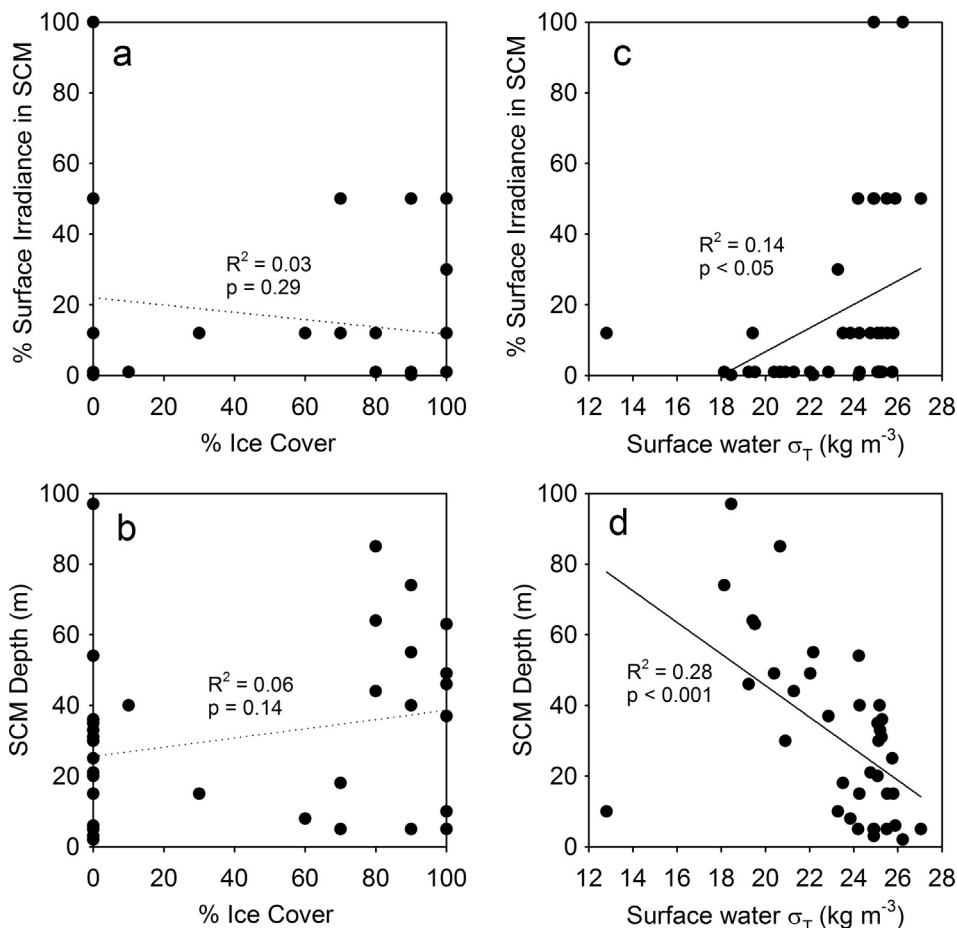
Fig. 10. Ratios of total (> 2 μm) phytoplankton carbon (total phyto C), total chlorophyll *a* (chl *a*), and total particulate biogenic silica (bSi) within the SCM over the five oceanographic domains. (a) ratio of phyto C:chl *a* (b) ratio of bSi:phyto C. The average ratio (± 1 SE) is based upon data from all full-profile stations for each domain. Data for chl *a* taken from Varela et al. (2013) and data for bSi from Wyatt et al. (2013).

coccoids fraction (2–8 μm) averaged 1.66 ± 0.24 μg C L^{-1} for the BS-CB domain, agreeing well with that of 1.1 ± 0.2 μg C L^{-1} for the < 10 μm fraction in the Canada Basin (Booth and Horner, 1997). Diatom C of 0.86 ± 0.38 μg C L^{-1} and dinoflagellate C of 1.59 ± 0.42 μg C L^{-1} were of the same order as biomass of the unidentified flagellate/coccoid (2–8 μm) fraction in this study, but somewhat lower than the measurements of 4.5 μg C L^{-1} and 2.7 μg C L^{-1} respectively observed by Coupel et al. (2012). The C biomass of unidentified flagellate/coccoids (2–8 μm) in the BS-CB was ~26% of that observed in the BE-CH, whereas combined C biomass of diatoms and dinoflagellates represented only ~3% of that in the BE-CH domain. This very low contribution of diatoms and dinoflagellates to total C in the BS-CB is consistent with previous findings showing that the > 5 μm fraction contributed < 27% of new production, nitrate uptake, and total chl *a* (Varela et al., 2013, Wyatt et al., 2013). Concentrations of bSi averaged only ~4% of those observed in the BE-CH (Wyatt et al., 2013), consistent with our maximum abundances of *Chaetoceros* spp. of only ~5% of those observed in the BE-CH. Few other diatom genera were observed in the BS-CB, with abundances for various species of *Chaetoceros* of a similar order of magnitude to those observed by Joo et al. (2012). Our observations support previous studies identifying the BS-CB as an oligotrophic environment numerically dominated by nanophytoplankton and picophytoplankton (Booth and Horner, 1997; Gosselin et al., 1997).

Fewer records of phytoplankton assemblages are available for the CAA. Ardyna et al. (2011) reported relative abundance, as size-fractionated chl *a*, for several taxa during summer 2005 in extended Arctic transects that included the CAA. Flagellates contributed ~50% on average to the abundance of total protist cells > 2 μm, whereas diatoms varied from < 10% at some stations to > 60% at others (average ~30%) and dinoflagellates contributed only ~2% (Ardyna et al.,

offshore stations in the Beaufort Sea in summer 2009. Total nano- and microphytoplankton C averaged 4.70 ± 0.83 μg C L^{-1}, a value within the summer ranges of 1.9 μg C L^{-1} for the SCM in the Canada Basin in 1994 (Gosselin et al., 1997), and 9.2 ± 7.6 μg C L^{-1} for the Beaufort Sea SCM in 2009 (Coupel et al., 2015). The unidentified flagellates/


Fig. 11. Relationships between % ice cover and (a) % surface irradiance within the SCM, and (b) the depth of the SCM. Relationships between surface water σ_T and (c) % surface irradiance within the SCM, and (d) depth of the SCM. Dotted line represents non-significant linear regression (p > .05) and solid line represents significant regression (p < .05). Data points for ice cover and σ_T of represent surface water properties for full-profile stations (see Tables 1 and 2).
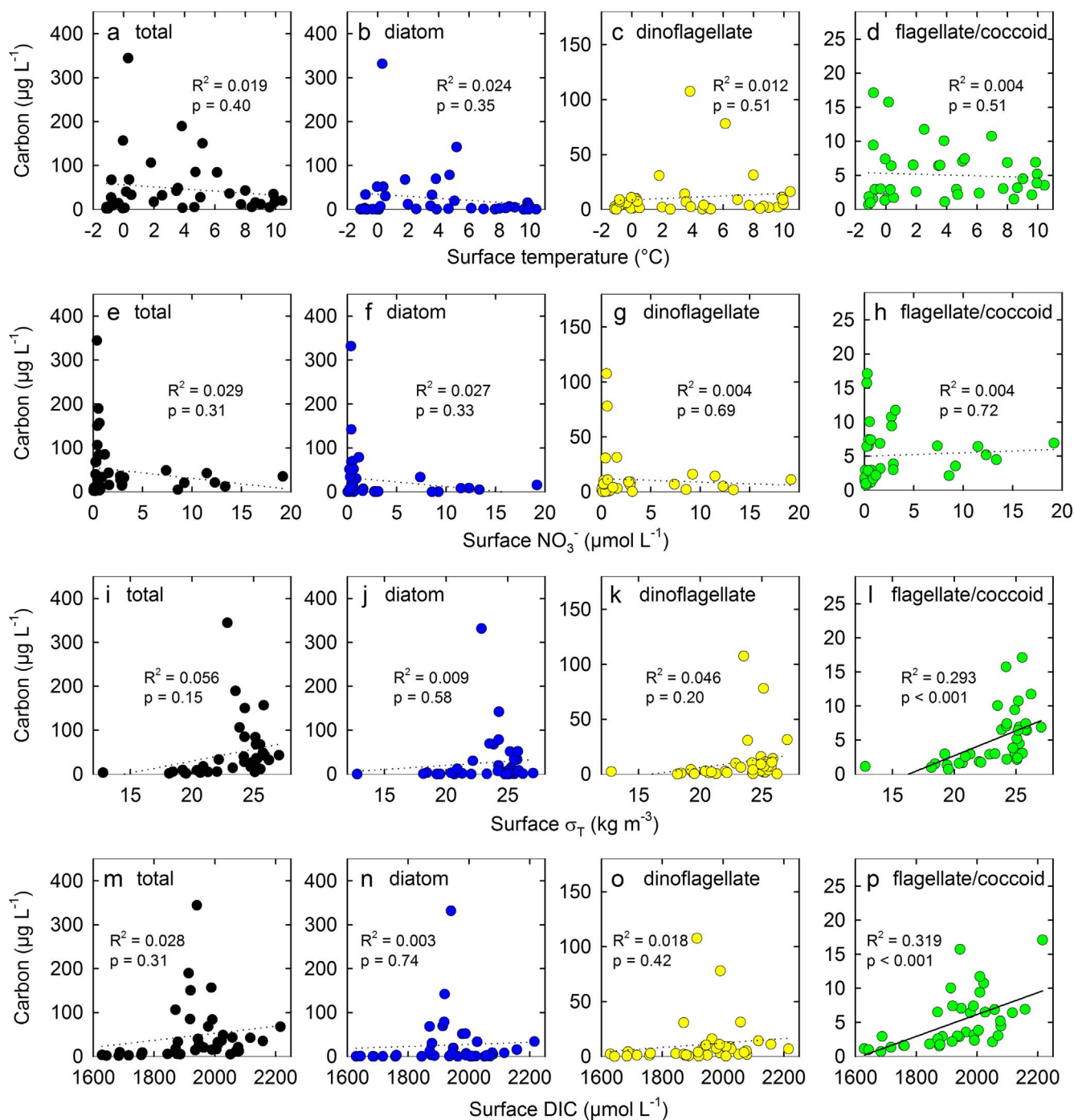
Fig. 12. Relationships between carbon biomass (C) of major taxonomic groups of phytoplankton (> 2 μm) within the SCM, and surface temperature (a, b, c, d), surface NO_3^- (e, f, g, h), surface σ_T (i, j, k, l) and surface DIC (m, n, o, p) across the five oceanographic domains. Total = C in total nano- and microphytoplankton. Dotted line represents non-significant linear regression (p > .05) and solid line represents significant regression (p < .05). Data points represent surface water properties for full-profile stations (see Table 2).

2011). Our abundance data for the CAA domain were similar, with ~64% unidentified flagellates/coccoids (2–8 μm), ~28% diatoms and ~3% dinoflagellates. Our measurement of total nano- and microphytoplankton C in the CAA was similar to but more variable (97.9 ± 53.5 μg C L^{-1}) than that in the BE-CH, whereas C biomass levels of unidentified flagellate/coccoids (2–8 μm) and dinoflagellates were much lower than in the BE-CH. The CAA domain was characterized by the high spatial variability in diatom C biomass, with a

maximum estimate of ~332 μg C L^{-1} at station CAA-10. These observations are consistent with high and variable bSi concentrations and with total chl *a*, nitrate uptake and new production dominated by the > 5 μm size fraction (Varela et al., 2013, Wyatt et al., 2013). In late summer and autumn, large areas of the high Arctic including the CAA have been characterized either as oligotrophic, dominated by eukaryotic picophytoplankton (< 2 μm) and unidentified nanoflagellates (2–20 μm), or as eutrophic, dominated by centric diatoms, such as

Table 6

Estimates of C quota per cell for a range of representative taxa observed during this study. Carbon estimates using the protist and diatom specific C:vol equations given by Menden-Deuer and Lessard (2000) were compared with those using the single equation adopted by Montagnes et al. (1994). The percent difference in C estimates between the two approaches is given in the final column.

Taxon	Approximate cell volume (µm³)	C quota (pg C cell^{-1})			Percent difference between C estimates using Menden-Deuer & Lessard (2000) vs. Montagnes et al. (1994) (%)
		Montagnes et al. (1994).	Menden-Deuer & Lessard (2000).		
		One equation for all protists	Equation for protists excluding diatoms	Equation for diatoms only	
Flagellate 2–5 µm	15	1.6	2.8		+72
Flagellate 5–8 µm	150	15.6	23.9		+53
Cryptophyceae	300	31.1	45.8		+47
Dinoflagellate e.g. *Gymnodinium* spp.	500	51.5	73.9		+43
Small diatom e.g. *Fragilariopsis nana*	16	1.7		2.7	+60
Medium diatom e.g. *Pauliella taeniata*	1000	102		78.1	−24
Medium diatom e.g. *Thalassiosira* spp.	10,000	1003		505	−50
Large diatom e.g. *Corethron hystrix*	60,000	5924		2160	−64

Chaetoceros spp. (Ardyna et al., 2011), and our data support these observations.

Our study did not include stations in the North Water Polynya (NOW) of the BB-LS domain, a highly productive area in the north of Baffin Bay (e.g. Mostajir et al., 2001; Vidussi et al., 2004; Garneau et al., 2007). Mostajir et al. (2001) also included surface stations further south in Baffin Bay that were more comparable with stations in our BB-LS domain, although their study was carried out in fall 1999 with samples taken only from the ocean surface. Our total nano- and microphytoplankton abundance for the BB-LS varied between 0.56 and 11.2 × 10⁶ cells L^{-1}, with abundances in Baffin Bay itself (i.e. not including the Labrador Sea) of between 2 and 4 × 10⁶ cells L^{-1}. This is in reasonable agreement with abundances of 0.81 to 4.35 × 10⁶ L^{-1} for cells < 20 µm in size reported by Mostajir et al. (2001) for Baffin Bay (not including the NOW region). Total phytoplankton C (> 2 µm) averaged 64.9 ± 14.9 µg C L^{-1} in the BB-LS in our study, which was much lower than in the BE-CH and CAA domains. Unidentified flagellates/coccoids (2–8 µm) contributed 9.6 ± 1.8 µg C L^{-1} of this total, a greater C biomass than in other domains. Previous studies have shown that the > 5 µm size fraction contributed > 50% of total chl *a*, new production and nitrate uptake (Varela et al., 2013, Wyatt et al., 2013) in the BB-LS, with bSi averaging < 50% of concentrations observed in the CAA (Wyatt et al., 2013). Our observations for the BB-LS support the notion of a diverse nano- and microphytoplankton summer assemblage with a lower diatom C biomass than in the CAA. The greater relative influence of unidentified flagellates/coccoids (2–8 µm), dinoflagellates and cryptomonads in the BB-LS could also be linked to lower summer concentrations of Si(OH)₄ in the sector of this domain that we studied (Varela et al., 2013). Blooms of *Phaeocystis* spp. have been shown to be a characteristic feature further south in the Labrador Sea (Fragoso et al., 2016, 2017) and it has been speculated that variations in Si* (Si(OH)₄ minus NO₃⁻ concentrations) may be involved in the competition between *Phaeocystis* and diatoms in this area (Fragoso et al., 2016, 2017). Our observations of high abundance of *Phaeocystis* spp. at station LS-7 in the Labrador Sea, combined with relatively low concentrations of Si(OH)₄ in the BB-LS (Varela et al., 2013) are consistent with this notion.

4.4. Overview of large-scale variability in nano- and microphytoplankton

The C biomass of unidentified flagellates/coccoids (2–8 µm) was relatively low and varied ~6-fold among domains, whereas average diatom and dinoflagellate C biomass varied ~100 fold and ~30-fold respectively. In the BE-CH and CAA, diatoms and dinoflagellates together contributed > 80% of total nano- and microphytoplankton C biomass. Thus, large-scale spatial variability of total C was driven by the abundance of these larger cells. Despite their relatively low C biomass, the unidentified flagellate/coccoid (2–8 µm) fraction provided a greater proportion of total within the less productive ESNP and BS-CB domains where they contributed ~27 and 39% to total C, respectively. With potentially higher intrinsic growth rates under low nutrient conditions relative to larger cells, and efficient grazing by heterotrophic protists, these smaller cells may contribute significantly to fixation, cycling and trophic transfer of C in these oligotrophic areas.

The diatoms *Thalassiosira* spp. and *Chaetoceros* spp. were the dominant taxa driving major variations in total phytoplankton C (> 2 µm) among Arctic domains. This observation is consistent with the findings of Poulin et al. (2011) who provided a pan-Arctic review of historical taxonomic records of phytoplankton presence. They indicated that the dominant taxa in the Canadian and Alaskan Arctic were centric diatoms of the genera *Thalassiosira* and *Chaetoceros*, and pennate diatoms of the genera *Cylindrotheca* and *Fragilariopsis*. The most significant dinoflagellate genus recorded by Poulin et al. (2011) was *Protoperidinium*, present in the Scandinavian and Russian Arctic, but not in the Canadian Arctic. *Protoperidinium* spp. were observed sporadically in the present study, but were considered to be heterotrophic forms (see Appendix). Our observations of the dominant athecate genera *Gymnodinium* and *Gyrodinium* contrast with the review of Poulin et al. (2011) that did not mention the *Gymnodinium* genus. It is not known whether this difference results from temporal shifts in dominant genera as a result of environmental change in Arctic waters, or whether fragile athecate dinoflagellates were under-represented by certain sampling and preservation methods in the historical record. It is notable however, that our observations of high abundance of *Gymnodinium* spp. in the BE-CH were corroborated by the study of Joo et al. (2012) from the same period as our study. Due to limitations of light microscopy, we did

not provide detailed taxonomical information on nanophytoplankton, and molecular techniques provide tremendous promise for examining the diversity of the pico- and nanophytoplankton diversity (e.g. Poulin et al., 2011).

Several taxa were recorded in low abundance and did not contribute significantly to total nano- and microphytoplankton C, but their presence appeared to be associated with particular domains or water masses. Cryptomonads, for example, were present in lower abundance in Arctic than in Subarctic domains, whereas silicoflagellates were more abundant in Arctic regions such as BS-CB. Elevated abundances of *Phaeocystis* spp. were mainly associated with the Labrador Sea, whereas the chlorophyceaen *Chlamydomonas* sp. was associated more with western domains (ESNP and BE-CH), and the prasinophyceaens *Pyramimonas* spp. more prominent to the east. Other small chlorophyceaens and prasinophyceaens could have been included in our unidentified flagellate/coccoid (2–8 μm) category, and therefore we must be cautious in extrapolating spatial patterns of smaller cells (2–8 μm) enumerated using light microscopy. Based on molecular techniques, small prasinophyceaens such as *Micromonas* spp. appear to have a more pan-Arctic distribution (Lovejoy et al., 2007) than implied by the *Pyramimonas* spp. observed in our study, and other small phytoplankton have been shown to be cold-adapted and endemic to Arctic waters (e.g. Lovejoy et al., 2007).

Phytoplankton growth has been shown to be limited by iron in central ESNP waters (e.g. Boyd et al., 1996), by irradiance, nitrate and iron in late summer in the Beaufort Sea (Taylor et al., 2013), but enhanced by upwelling of nutrients into shallow water in the BE-CH (Carmack and McLaughlin, 2011; Varela et al., 2013). Given the large spatial scales involved and the variability in oceanographic features within and among domains, it is perhaps not surprising that there is little evidence for any single physical or chemical variable driving spatial changes in nano-and microphytoplankton C. The depth of the SCM varied considerably across the study area (Fig. 2, Tables 1 and 2) but was deeper in the BS-CB and CAA domains where ice cover was greatest. However, relationships were insignificant between % ice-cover and both average irradiance within the SCM (Fig. 11a), and the depth of the SCM (Fig. 11b). By contrast, a weak but significant positive relationship (p < .05) was evident between density of surface water and average irradiance in the SCM (Fig. 11c), and a stronger inverse relationship (p < .001) between surface water density and the depth of the SCM (Fig. 11d). Our data are therefore consistent with a deeper SCM in areas of reduced surface σ_T and increased stratification, with consequentially reduced irradiance within the SCM, particularly in the BS-CB domain.

Stratification of Arctic surface waters has increased in recent years as a result of sea-ice melt and increased riverine input (McLaughlin and Carmack, 2010). In some areas, this increased stratification dampens vertical mixing of the upper water column with a consequential deepening of the nitracline and the SCM (McLaughlin and Carmack, 2010). This has been associated with a concomitant decrease in the abundance of nanophytoplankton and an increase in the relative contribution of picophytoplankton (Li et al., 2009). In the present study, both in surface water and within the SCM, temperature was relatively invariant across the BE-CH, BS-CB, CAA and BB-LS domains. Indeed, there was no evidence of a significant relationship between surface temperature and C biomass of the major taxonomic groups (Fig. 12a–d). Similarly, surface water NO_3^- showed no significant relationship (Fig. 12e–h) with the C content of major taxonomic groups. This presumably results from low nitrate concentrations being a feature of both reduced vertical supply to stratified surface waters – with consequently low phytoplankton biomass (e.g. BS-CB) – and of high biological drawdown with consequently high biomass (e.g. BE-CH). The significant relationship between surface

water σ_T and depth of SCM (Fig. 11d), did not extend to a relationship between surface water σ_T and total C biomass, or the C biomass of diatoms or dinoflagellates (Fig. 12i–k). However, a significant relationship (p < .001) was evident (Fig. 12l) between surface water σ_T and the C biomass of unidentified flagellates/coccoids (2–8 μm). Similarly, relationships between surface water DIC and the C biomass of major taxonomic groups (Fig. 12m–p) showed a significant relationship (p < .001, Fig. 12p) only with unidentified flagellates/coccoids (2–8 μm). It is not known whether this represents some form of direct effect of lower DIC, or simply results from the relatively conservative relationship between DIC and salinity/density. Our observations support the contentions of Li et al. (2009), in suggesting that the deeper SCM (and decreased irradiance within the SCM) associated with surface water stratification, also appears to be associated with a significant decrease in at least the 2–8 μm size-fraction of the nanophytoplankton assemblage (2–20 μm). Density stratification clearly plays a key role in the vertical mixing that shapes phytoplankton communities in the Beaufort Sea, CAA and Baffin Bay as suggested by Ardyna et al. (2011).

4.5. Spatial variability in C:chl a and bSi:C ratios in nano- and microphytoplankton

The wide range of phyto C:chl *a* ratios, from 31 in BS-CB to 51–150 in the other domains, agrees with the modelled range of 20 to > 160 g C g chl a^{-1} between latitudes of 0° and 60°N (Taylor et al., 1997), the measured range of 19–150 g C g chl a^{-1} in a North Pacific coastal environment (Welschmeyer and Lorenzen, 1984), and the range of ∼ 10 and > 200 g C g chl a^{-1} measured in phytoplankton cultures (Geider, 1987; Taylor et al., 1997). Ratios of C:chl *a* appear to be driven principally by complex interactions between irradiance, nutrients and temperature (Geider, 1987; Taylor et al., 1997), but the impact of these factors on ratios over the wide geographical area covered by the present study is unknown. Although some evidence of high C:chl *a* ratios have been reported at low temperatures in Arctic waters (review of Geider, 1987), our data show a wide range of ratios across a variety of Arctic domains where temperature is relatively invariant. Minimum phyto C:chl *a* ratios were observed in the deep SCM of the BS-CB domain, as has been noted previously (Booth and Horner, 1997; Sherr et al., 2003), and may be indicative of phytoplankton acclimated to low irradiance (Smith and Sakshaug, 1990; Sherr et al., 2003).

Ratios of bSi:phyto C averaged ∼ 0.22 to 0.49 across domains, somewhat higher than the bSi:C range (average 0.13) given by Brzezinski (1985) for cultured diatoms. However, our observed range may have been influenced by the low POC:PON ratios observed in certain regions (Crawford et al., 2015), and by variations in the presence of non-siliceous taxa among domains. Baines et al. (2010) observed bSi per unit cell volume to be ∼ 6-fold higher for diatoms in the $Si(OH)_4$ rich waters of the Antarctic Zone of the Southern Ocean, compared to $Si(OH)_4$ poor waters of the eastern equatorial Pacific. Similarly, observations of lower ratios of bSi:phyto C in our eastern domains could be consistent with lower summer concentrations of $Si(OH)_4$ in these areas (Varela et al., 2013), potentially constraining the growth and/or silicification of some diatom species. Caution should be exercised in interpretation of these data because of the potential contribution of detrital Si to the bSi:C ratio (Krause et al., 2010). Clearly, however, the plasticity in both bSi:phyto C and phyto C:chl *a* ratios across these broad oceanographic domains has implications for biogeochemical processes, modelling, and remote sensing studies.

4.6. Potential biases in estimation of C from cellular volume

The use of constant C:vol conversion factors over large ranges in

phytoplankton size can result in systematic errors in biomass estimates (Menden-Deuer and Lessard, 2000). In the present study, estimates of cellular C for each phytoplankton taxon were calculated using separate equations for diatoms and for all other protists (Menden-Deuer and Lessard, 2000). In order to examine potential biases when comparing C estimates with other studies, estimates of C calculated from a single equation for all protists (Montagnes et al., 1994) were compared with our estimates for several representative taxa in Table 6. The choice of equation clearly has a significant impact on the estimated C quota per cell, and this varies both with cell size and taxonomic group (Table 6). Cellular C quotas estimated using the Menden-Deuer and Lessard (2000) equations were 43–72% higher than using the Montagnes et al. (1994) equation for typical flagellates and dinoflagellates, 60% higher for small diatoms, and between 24 and > 60% lower for medium and large diatoms (Table 6) (and even lower for larger diatoms, data not shown).

Because the relative proportion of taxonomic groups varied across domains, variations in C quota per cell also have important implications for estimates of total nano- and microphytoplankton C. In the ESNP and BS-CB domains, where the relative contribution of unidentified flagellates/coccoids (2–8 μm) was greater, average total phytoplankton C (> 2 μm) estimated using the Montagnes et al. (1994) equation was ~1–12% lower than using the equations of Menden-Deuer and Lessard (2000). In the BB-LS and BE-CH domains, a more balanced mix of diatoms, dinoflagellates and unidentified flagellates/coccoids (2–8 μm) was present, and the average total C calculated using the Montagnes et al. (1994) equation was ~16–33% higher than using Menden-Deuer and Lessard (2000) equations. In the CAA domain, where the relative contribution of diatoms was greatest, the average total C calculated using the Montagnes et al. (1994) equation was almost a factor of 2 higher than using the Menden-Deuer and Lessard (2000) equations. The present study has adopted the most appropriate equations that take into account variations in C density between diatoms and other autotrophic protists (Menden-Deuer and Lessard, 2000). However, allometry ignores species-specific variability with the final aim of providing average estimates for comparative purposes (Menden-Deuer and Lessard, 2000). Our phytoplankton C estimates will therefore be influenced by the taxonomic similarity between assemblages in each domain and the taxa represented in the study of Menden-Deuer and Lessard (2000). These considerations demonstrate that the C:vol equations adopted should be a major consideration when comparing C biomass estimates both historically and in future studies.

5. Conclusions

Temporal and spatial comparisons of phytoplankton assemblages among studies can be hampered by methodological, taxonomic and size category inconsistencies. Our study attempted to minimize some of these issues by adopting a consistent methodology and approach to provide a snapshot of nano- and microphytoplankton assemblages across five Subarctic and Arctic domains during the summers of 2007 and 2008.

Average abundance of nano- and microphytoplankon varied ~10-fold, and total C biomass varied ~20-fold among domains. Spatial variation in biomass was driven mainly by diatoms and dinoflagellates, together accounting for 55% to > 80% of total phytoplankton C (> 2 μm) in all domains except for the oligotrophic BS-CB.

Estimates of C quota for various taxa were highly sensitive to the C:vol equations adopted, with a consequential impact on estimates of total phytoplankton C (> 2 μm). Diatom-rich areas are particularly susceptible to uncertainties, because of specific issues with allometric scaling of C:vol equations.

Variations in taxonomic composition in each domain led to significant variations in phyto C:chl *a* and bSi:phyto C ratios, with important implications for modelling and biogeochemical studies in these areas.

The depth of the SCM, and to some extent the taxonomic composition of phytoplankton within it, were shown to be significantly influenced by the density of surface water. These observations support recent studies highlighting the role of thinning and melting sea ice in shaping phytoplankton assemblages, with potential consequences for primary productivity and transfer of C to higher trophic levels.

Appendix

Samples for identification of nano- and microphytoplankton were collected from the depth of the subsurface chlorophyll maximum (SCM) where present (see Table 1 for sampling depths). Data correspond to cruises 2007–19, 2007–20, and 2008–02 in the summers of 2007 and 2008 in Arctic and Subarctic Seas (see Fig. 1 and Table 1 for station and domain locations). Additional samples from surface stations were taken in the upper 2–10 m of the water column (see Table 1); these surface data are presented here only (and nowhere else in this paper) to support other chemical and biological data for surface stations shown in Varela et al. (2013). Note that in contrast to the text, tables and a few figures, abundance here is expressed in cells $L^{-1} \times 10^3$ because of the many uncommon taxa present at low abundances.

X denotes species recorded as present in low abundance but not enumerated.

*Denotes heterotrophic dinoflagellates not included in phytoplankton C biomass estimates.

Appendix Table 1
Abundance of phytoplankton taxa at stations in the Eastern Subarctic North Pacific (ESNP) domain.

ESNP domain		Abundance (cells L^{-1} × 10^3)											
		Stations sampled at the SCM									Surface Stations		
		NP-5	NP-6	NP-8	NP-9	NP-12	NP-13	NP-14	BCL-2	BS-5	UN-7	UN-4	UN-2
Diatoms (Bacillariophyceae)	*Actinocyclus tenuissimus* Cleve				X								
	Asteromphalus sp.				5.7								
	Chaetoceros brevis Schütt												151.1
	Chaetoceros convolutus Castracane	X					17.1	X					5.7
	Chaetoceros debilis Cleve						5.1						592.9
	Chaetoceros diadema (Ehrenberg) Gran (resting spores)												2.9
	Chaetoceros didymus Ehrenberg												14.3
	Chaetoceros similis Cleve	X											
	Chaetoceros gelidus Chamnansinp, Li, Lundholm & Moestrup						17.1						131.1
	Corethron hystrix Hensen				2.9	2.1							11.4
	Cylindrotheca closterium (Ehrenberg) Reimann & Lewin					190.3		3.4	5.7	47.0	4.3	5.7	
	Fragilariopsis cylindrus (Grunow ex Cleve) Frenguelli				39.9				5.7	10.7			
	Fragilariopsis cylindrus/nana complex						5.1						
	Fragilariopsis oceanica (Cleve) Hasle				X								X
	Neodenticula seminae (Simonsen &.Kanaya) Akiba & Yanagisawa	1.7		1.7	14.3		1.7						X
	Plagiotropis sp.				X								
	Proboscia cf. *alata*				2.9								
	Proboscia cf. *inermis*						3.4						
	Proboscia sp.					2.1							
	Pseudo-nitzschia obtusa (Hasle) Hasle & Lundholm												X
	Pseudo-nitzschia spp.	12.0		6.8	14.3	10.7	71.8	1.7					25.7
	Rhizosolenia hebetata f. *semispina* (Hensen) Gran											11.4	11.4
	Rhizosolenia styliformis Brightwell	X											
	Rhizosolenia sp.			5.1				X					
	Thalassiosira lineata Jousé												X
	Thalassiosira pacifica Gran & Angst												X
	Thalassiothrix longissima Cleve & Grunow				X		X						
	Unidentified centric diatoms < 15 µm						3.4		2.9			2.9	42.8
	Unidentified centric diatoms > 15 µm			1.7	2.8	2.1				2.1	17.1		11.4
	Unidentified pennate diatoms								2.9				
Dinoflagellates (Dinophyceae)	*Alexandrium* sp.										4.3	2.9	
	Amphidinium spp.				5.7				1.4				
	Dinophysis norvegica Claparède & Lachmann				X								
	Gymnodinium spp.	18.8	25.7	22.2	82.7	32.1	12.0	70.1	31.3	55.6	124.0	45.6	8.6
	Gyrodinium fusiforme Kofoid & Swezy[*]				X								
	Gyrodinium spp.		1.7	3.4	8.6		3.4			10.7	4.3	14.3	
	Prorocentrum minimum (Pavillard) Schiller	1.7			X								
	Prorocentrum sp.				2.9								
	Protoperidinium cf. *brevipes*[*]				X								
	Protoperidinium bipes (Paulsen) Balech[*]					2.1	X	1.7				5.7	
	Tripos muellerii Bory	1.7											
Prymnesiophyceae	*Phaeocystis* spp. (single cells)					12.8	53.0	23.9				1180	
	Phaeocystis spp. (in colony)						X						X
Unidentified flagellates/coccoids 2–8 µm	2–5 µm	663.6	371.1	636.2	578.6	831.6	376.3	557.6	243.7	825.2	1689	689.8	655.6
	5–8 µm	42.8	29.1	77.0	165.3	79.1	63.3	65.0	74.1	265.1	466.1	42.8	96.9
Cryptomonads (Cryptophyceae)	*Plagioselmis* cf. *prolonga* & *Teleaulax* cf. *amphioxeia*										684.1		
	Cryptomonad cells	8.6	22.2	35.9	62.7	66.3	53.0	73.5	152.5	228.8		307.9	245.1
Prasinophyceae	*Pyramimonas* spp.										21.4		14.3
Chrysophyceae	*Dinobryon balticum* (Schütt) Lemmermann									6.4	21.4		37.1
Euglenophyceae	Euglenid cells						1.7				12.8		X
Silicoflagellates (Dictyochophyceae)	*Dictyocha speculum* Ehrenberg							1.7			4.3		X
Chlorophyceae	*Chlamydomonas* sp.				3.4		1.7		1.4	4.3	8.6		

Appendix Table 2
Abundance of phytoplankton taxa at stations in the Bering and Chukchi Seas (BE-CH) domain. No surface stations were sampled within this domain.

		Abundance (cells $L^{-1} \times 10^3$)				
		Stations sampled at the SCM				
BE-CH Domain		SLIP-4	UTBS-1	UTN-4	CCL-4	BC-2
Diatoms (Bacillariophyceae)	*Actinoptychus senarius* (Ehrenberg) Ehrenberg				X	
	Chaetoceros debilis Cleve	6.1			25.7	
	Chaetoceros diadema (Ehrenberg) Gran			32.8		
	Chaetoceros gelidus Chamnansinp, Li, Lundholm & Moestrup	11.0	215.9	166.8	518.8	880.8
	Chaetoceros spp.	2.4				
	Chaetoceros sp. (resting spores)	4.9				
	Coscinodiscus wailesii Gran & Angst			2.9		
	Cyclotella sp.				X	
	Cylindrotheca closterium (Ehrenberg) Reimann & Lewin		2.1	5.7	14.3	14.3
	Dactyliosolen sp.			1.4		
	Diploneis sp.				X	
	Fragilariopsis cylindrus (Grunow ex Cleve) Frenguelli	20.8			5.7	
	Fragilariopsis nana (Steemann Nielsen) Paasche					2.9
	Gyrosigma/Pleurosigma sp. complex				X	
	Leptocylindrus danicus Cleve			14.3		
	Melosira sp.				X	
	Navicula algida Grunow				X	
	Navicula directa (Smith) Ralfs				X	
	Navicula sp.				X	2.9
	Nitzschia frigida Grunow				34.2	
	Nitzschia spp.				2.9	2.9
	Nitzschia sp. in ribbon like-colony				11.4	
	Odontella aurita (Lyngbye) Agardh				X	
	Pauliella taeniata (Grunow) Round & Basson				X	635.7
	Plagiotropis sp.					2.9
	Pseudogomphonema cf. *kamtschaticum*				X	
	Pseudo-nitzschia obtusa (Hasle) Hasle & Lundholm					X
	Pseudo-nitzschia spp.					17.1
	Rhizosolenia hebetata f. *semispina* (Hensen) Gran	1.2				
	Thalassiosira spp.				62.7	
	Thalassiosira sp. in resting spores				14.3	
	Thalassiosira antarctica var. *borealis* Fryxell, Doucette & Hubbard resting spores				X	5.7
	Thalassiosira cf. *hyalina* resting spores				X	X
	Unidentified centric diatoms > 15 µm		4.3	5.7	2.9	25.7
	Unidentified pennate diatoms			1.4	2.9	
	Unidentified resting spores				2.9	
Dinoflagellates (Dinophyceae)	*Alexandrium* sp.	1.2			5.7	
	Amphidinium spp.				X	2.9
	Gymnodinium spp.	7.3	34.2	28.5	14.3	37.1
	Gyrodinium fusiforme Kofoid & Swezy[*]				2.9	5.7
	Gyrodinium pepo (Schütt) Kofoid & Swezy[*]			X	X	
	Gyrodinium spirale (Bergh) Kofoid & Swezy[*]			X		
	Gyrodinium spp.	1.2	2.1	12.8		
	Peridiniella catenata (Levander) Balech (in colony)				11.4	
	Protoperidinium bipes (Paulsen) Balech[*]	1.2				
	Protoperidinium sp.[*]		8.6			
	Unidentified cysts		2.1			
	Unidentified cells					2.9
Prymnesiophyceae	*Phaeocystis* spp. (single cells)	3.7				
	Phaeocystis spp. (in colony)			35.6		
	Unidentified coccolithophores			1.4		
Unidentified flagellates/coccoids 2–8 µm	2–5 µm	289.5	1035	916.5	430.4	869.4
	5–8 µm	46.4	96.2	112.6	168.2	236.6
Cryptomonads (Cryptophyceae)	Cryptomonad cells	78.2	34.2	49.9	22.8	91.2
Prasinophyceae	*Pyramimonas* spp.				2.9	
Chrysophyceae	*Dinobryon balticum* (Schütt) Lemmermann		10.7	1.4	2.9	
Chlorophyceae	*Chlamydomonas* sp.					8.6
Unidentified	Unidentified cells.		4.3			

Appendix Table 3
Abundance of phytoplankton taxa at stations in the Beaufort Sea and Canada Basin (BS-CB) domain.

BS-CB Domain		Abundance (cells L^{-1} × 10^3)														
		Stations sampled at the SCM										Surface stations				
		BI-2	CB-29	CB-2a	CB-4	CB-9	CB-11b	CB-15	CB-21	MK-1	BFB-5	MK-3	MK-1	CB-28aa	BL-4	BFB-6
Diatoms (Bacillariophyceae)	*Actinoptychus senarius* (Ehrenberg) Ehrenberg												2.1			
	Chaetoceros decipiens Cleve										2.9					
	Chaetoceros debilis Cleve			1.9		2.4										
	Chaetoceros gelidus Chamnansinp, Li, Lundholm & Moestrup		1.9			41.5	2.4	7.0	14.5			3.4	17.1	2236	128.3	
	Chaetoceros spp.										7.1			226.6		
	Cylindrotheca closterium (Ehrenberg) Reimann & Lewin							0.8		1.7		3.4	4.3	8.6	5.1	3.4
	Fragilariopsis nana (Steemann Nielsen) Paasche					3.7	1.2		3.4							
	Fragilariopsis cylindrus/ nana complex							5.4						8.6		
	Nitzschia spp.								1.7							
	Pseudo-nitzschia spp.					3.7								4.3		
	Thalassiosira cf. *hyalina*													42.7	13.7	
	Thalassiosira spp.								1.7					136.8	3.4	
	Unidentified centric diatoms < 15 µm					1.2						1.7			1.7	
	Unidentified centric diatoms > 15 µm					3.7				10.3		1.7	4.3	17.1		
Dinoflagellates (Dinophyceae)	*Alexandrium* sp.					1.2						1.7	6.4		3.4	1.7
	Amphidinium spp.							0.8				1.7	2.1		1.7	X
	Gymnodinium spp.	12.4	7.6	12.4	41.0	7.3	20.8		2.6	12.0	12.8	32.5	77.0		29.1	27.4
	Gyrodinium spp.			2.9	5.1	2.4	2.4							4.3	3.4	
	Protoperidinium cf. *brevipes*[*]												2.1			1.7
	Scrippsiella sp.				1.7											
	Unidentified cysts											3.4				
	Unidentified cells			1.0												
Prymnesiophyceae	Unidentified cells															5.1
Unidentified flagellates/ coccoids 2–8 µm	2–5 µm	360.1	234.7	147.3	364.3	278.5	272.4	162.5	188.1	340.4	538.8	786.8	1261	2476	834.7	773.1
	5–8 µm	13.3	18.1	20.9	56.4	20.8	30.5	5.4	11.1	12.0	37.1	131.7	81.2		138.5	246.3
Cryptomonads (Cryptophyceae)	Unidentified cells			1.0	8.6	4.9	4.9	1.6	0.9	1.7		58.2	44.9	72.7	13.7	1.7
Prasinophyceae	*Pyramimonas* spp.		6.7		1.7	2.4					5.7	18.8	15.0	29.9	15.4	10.3
Chrysophyceae	*Dinobryon balticum* (Schütt) Lemmermann	1.9				2.4		2.3				97.5	8.6		171.0	
	Dinobryon sp.															37.6
Euglenophyceae	*Eutreptiella* sp.	1.9														
Silicoflagellates (Dictyochophyceae)	*Dictyocha speculum* Ehrenberg	1.0			3.4	2.4	1.2	0.8								
Chlorophyceae	*Chlamydomonas* sp.										1.4					
Unidentified	Unidentified cells														6.8	

Appendix Table 4
Abundance of phytoplankton taxa at stations in the Canadian Arctic Archipelago (CAA) domain.

		Abundance (cells L^{-1} × 10^3)						
		Stations sampled at the SCM						Surface Stations
CAA Domain		CAA-2	CAA-5	CAA-6	CAA-10	CAA-12	CAA-16	BE-2
Diatoms (Bacillariophyceae)	*Achnanthes* sp.		2.9				1.1	
	Actinocyclus sp.	2.1						
	Actinoptychus senarius (Ehrenberg) Ehrenberg	15.0						
	Chaetoceros convolutus Castracane				2.9			
	Chaetoceros cf. *furcellatus* Bailey		X					
	Chaetoceros cf. *laciniosus* Schütt				11.4	1.4		
	Chaetoceros gelidus Chamnansinp, Li, Lundholm & Moestrup	124.0	82.7	23.8	108.3	3.6	82.3	21.4
	Chaetoceros spp.					6.4	2.1	
	Cocconeis sp.					2.1		
	Coscinodiscus gigas Ehrenberg	X						
	Coscinodiscus sp.				2.9			
	Cylindrotheca closterium (Ehrenberg) Reimann & Lewin		X		X	10.0		
	Detonula confervacea (Cleve) Gran	8.6						
	Eucampia groenlandica Cleve		5.7					
	Fossula arctica Hasle, Syvertsen & von Quillfeldt	X	39.9		X			
	Fragilaria sp.		X					
	Fragilariopsis cylindrus (Grunow ex Cleve) Frenguelli		X		X			
	Fragilariopsis nana (Steemann Nielsen) Paasche			1.9		4.3	10.7	2.1
	Fragilariopsis oceanica (Cleve) Hasle	21.4	X		X	8.6		
	Fragilariopsis pseudonana (Hasle) Hasle					17.1		
	Gyrosigma/Pleurosigma sp. complex							X
	Leptocylindrus mediterraneus (Peragallo) Hasle	2.1						
	Licmophora sp.			1.9			X	X
	Navicula directa (Smith) Ralfs							X
	Navicula pelagica Cleve		X					
	Navicula vanhoeffenii Gran	36.3	X					
	Navicula sp.	2.1	2.9					
	Nitszchia cf. *promare*					2.9		
	Nitzschia spp.		14.3					
	Pauliella taeniata (Grunow) Round & Basson		X				50.2	
	Plagiotropis sp.							X
	Pseudogomphonema cf. *kamtschaticum*							2.1
	Pseudo-nitzschia obtusa (Hasle) Hasle & Lundholm		X					
	Pseudo-nitzschia spp.	2.1	X		17.1		1.1	1.1
	Thalassiosira cf. *hyalina*							2.1
	Thalassiosira nordenskioeldii Cleve	4.3	11.4					
	Thalassiosira spp.	100.5	X		770.0	10.7	10.7	1.1
	Thalassiosira antarctica var. *borealis* Fryxell, Doucette & Hubbard resting spores	59.9	X		X			
	Unidentified centric diatoms < 15 μm	2.1	8.6	1.0			2.1	1.1
	Unidentified centric diatoms > 15 μm	29.9	20.0		62.7	7.8	1.1	3.2
	Unidentified pennate diatoms					1.4		1.1
	Unidentified pennate diatoms in ribbon-like colonies	12.8	14.3					
Dinoflagellates (Dinophyceae)	*Alexandrium* sp.				2.9		1.1	
	Amphidinium spp.			3.8	5.7	0.7		
	Gymnodinium spp.	15.0	25.7	30.4	5.7	11.4	21.4	20.3
	Gyrodinium spp.					0.7		
	Protoperidinium depressum (Bailey) Balech[*]		X					
	Protoperidinium sp.[*]		X	1.0				
Prymnesiophyceae	*Phaeocystis* spp. (in colony)							78.0
Unidentified flagellates/coccoids 2–8 μm	2–5 μm	393.4	496.0	365.8	553.0	358.5	530.2	938.6
	5–8 μm	203.1	179.6	58.9	34.2	16.4	25.7	69.5
Cryptomonads (Cryptophyceae)	Unidentified cells	23.5	2.9	8.6		2.9	18.2	39.6
Prasinophyceae	*Pyramimonas* spp.		X	1.0				9.6
Chrysophyceae	*Dinobryon balticum* (Schütt) Lemmermann			202.4				
Silicoflagellates (Dictyochophyceae)	*Dictyocha speculum* Ehrenberg						1.1	41.7
Chlorophyceae	*Chlamydomonas* sp.							3.2

Appendix Table 5

Abundance of phytoplankton taxa at stations in the Baffin Bay and Labrador Sea (BB-LS) domain. No surface stations were sampled within this domain.

| | | Abundance (cells L^{-1} × 10^3) | | | | | | | |
| | | Stations sampled at the SCM | | | | | | | |
BB-LS Domain		LS-2	LS-4	LS-7	BB-1	BB-5	BB-8	BB-10	BEW-11
Diatoms (Bacillariophyceaea)	*Achnanthes* sp.	1.2							
	Attheya septentrionalis (Østrup) Crawford	6.1							2.9
	Bacterosira bathyomphala (Cleve) Syvertsen & Hasle	31.8							
	Cerataulina pelagica (Cleve) Hendey	X							
	Chaetoceros debilis Cleve	36.7					11.4		
	Chaetoceros cf. *furcellatus* Bailey	X					17.1		
	Chaetoceros gelidus Chamnansinp, Li, Lundholm & Moestrup	44.0					875.1	498.9	
	Chaetoceros spp.	1.2	1.4		2.9	2.4		225.2	601.5
	Cylindrotheca closterium (Ehrenberg) Reimann & Lewin			82.7			2.9	45.6	17.1
	Fossula arctica Hasle, Syvertsen & von Quillfeldt						X		
	Fragilariopsis cylindrus (Grunow ex Cleve) Frenguelli	6.1		68.4			57.0	134.0	
	Fragilariopsis nana (Steemann Nielsen) Paasche					12.2		X	77.0
	Fragilariopsis cylindrus/nana complex					362.0		X	
	Fragilariopsis oceanica (Cleve) Hasle						14.3	48.5	11.4
	Fragilariopsis spp.	X							
	Leptocylindrus mediterraneus (Peragallo) Hasle					1.2		2.9	
	Licmophora sp.	X							
	Manguinea rigida (Peragallo) Paddock		2.9						
	Navicula pelagica Cleve	X							
	Nitzschia spp.							X	
	Pauliella taeniata (Grunow) Round & Basson	6.1							
	Plagiogrammopsis vanheurckii (Grunow) Hasle, von Stosch & Syvertsen								X
	Pseudo-nitzschia obtusa (Hasle) Hasle & Lundholm						X		
	Pseudo-nitzschia spp.		1.4			1.2	2.9	11.4	8.6
	Thalassiosira antarctica var. *borealis* Fryxell, Doucette & Hubbard	37.9							
	Thalassiosira cf. *hyalina*	X							
	Thalassiosira nordenskioeldii Cleve	20.8					48.5		
	Thalassiosira spp.	4.9		225.2			42.8	17.1	
	Thalassiosira antarctica var. *borealis* Fryxell, Doucette & Hubbard resting spores	X							
	Unidentified centric diatoms < 15 µm						5.7	270.8	17.1
	Unidentified centric diatoms > 15 µm	2.4					14.3		
	Unidentified pennate diatoms			11.4					5.7
	Unidentified pennate diatoms in ribbon-like colonies						39.9	5.7	
Dinoflagellates (Dinophyceae)	*Alexandrium* sp.		2.9			2.4			
	Amphidinium spp.	X		5.7					
	Dinophysis acuta/norvegica complex		1.4						
	Gymnodinium elongatum Hope		11.4						
	Gymnodinium cf. *verruculosum*		4.3						
	Gymnodinium spp.	17.1	225.2	91.2	11.4	59.9	14.3	116.9	74.1
	Gyrodinium cf. *formosum*[*]					14.7			
	Gyrodinium fusiforme Kofoid & Swezy[*]		1.4						
	Gyrodinium lachryma (Meunier) Kofoid & Swezy[*]		2.9						
	Gyrodinium pingue (Schütt) Kofoid & Swezy[*]							2.9	
	Gyrodinium spp.	X	14.3	2.9		3.7			
	Lebouridinium glaucum (Lebour) Gomez, Takayama, Moreira & Lopez-Garcia		1.4						
	Prorocentrum sp.					1.2			
	Protoperidinium bipes (Paulsen) Balech[*]	X				1.2			
	Protoperidinium depressum (Bailey) Balech[*]						X		
	Protoperidinium sp.[*]	X							
	Pyrophacus cf. *horologium*		5.7				2.9		
	Scrippsiella sp.							8.6	
	Unidentified cells		1.4						
Prymnesiophyceae	*Phaeocystis* spp. (single cells)				9299				
	Phaeocystis spp. (in colony)							114.0	
	Unidentified coccolithophores	1.2							
Unidentified flagellates/coccoids 2–8 µm	2–5 µm	294.4	1357	769.7	2873	1521	778.2	1257	2266
	5–8 µm	39.1	75.5	159.6	65.6	141.7	116.9	427.6	268.0
Cryptomonads (Cryptophyceae)	*Plagioselmis* cf. *prolonga*			325.0	627.1	97.7	74.1		193.8
	Plagioselmis cf. *prolonga* & *Teleaulax* cf. *amphioxeia*	4.9						248.0	
	Teleaulax cf. *amphioxeia*		29.9						
Prasinophyceae	*Pyramimonas* cf. *nansenii*					130.7			
	Pyramimonas spp.	3.7	5.7	111.1	88.4			5.7	108.3	196.7
Chrysophyceae	*Dinobryon balticum* (Schütt) Lemmermann		15.7						
Euglenophyceae	*Eutreptia* sp.					1.2			
	Unidentified cells	X	2.9						
Unidentified	Unidentified cells		1.4						
Silicoflagellates (Dictyochophyceae)	*Dictyocha speculum* Ehrenberg							2.9	
Unidentified	Unidentified cells						2.4	2.9	

Appendix Table 6
Abundance of phytoplankton taxa at stations excluded from the domain classification.

Excluded stations		Abundance (cells L^{-1} × 10^3)					
		Stations sampled at the SCM					Surface Stations
		AG-5	BL-2	NP-1	BL-1	BFB-7	BL-1
Diatoms (Bacillariophyceae)	*Attheya septentrionalis* (Østrup) Crawford		31.4			2.9	
	Chaetoceros concavicornis Mangin				1.1	5.7	
	Chaetoceros convolutus Castracane					2.9	
	Chaetoceros decipiens Cleve				5.3	2.9	
	Chaetoceros debilis Cleve					14.3	
	Chaetoceros eibenii Grunow				1.1	5.7	
	Chaetoceros gelidus Chamnansinp, Li, Lundholm & Moestrup		490.3		4.3	290.8	
	Chaetoceros spp.		273.7				
	Coscinodiscus sp.					2.9	
	Cylindrotheca closterium (Ehrenberg) Reimann & Lewin		2.9	25.7		2.9	
	Eucampia groenlandica Cleve		42.8				
	Fossula arctica Hasle, Syvertsen & von Quillfeldt		X				
	Fragilariopsis cylindrus (Grunow ex Cleve) Frenguelli			25.7		5.7	
	Fragilariopsis nana (Steemann Nielsen) Paasche		5.7		1.1		
	Fragilariopsis oceanica (Cleve) Hasle		325.0				
	Navicula sp.		2.9				
	Nitzschia spp.		2.9				
	Pauliella taeniata (Grunow) Round & Basson		2.9				
	Pseudo-nitzschia spp.		145.4		5.3	28.5	
	Thalassiosira anguste-lineata (Schmidt) Fryxell & Hasle		X				
	Thalassiosira spp.		134.0			X	
	Thalassiosira antarctica var. *borealis* Fryxell, Doucette & Hubbard resting spores		X				
	Unidentified centric diatoms < 15 μm		11.4			156.8	
	Unidentified centric diatoms > 15 μm		8.6				
	Unidentified pennate diatoms in ribbon-like colonies		119.7				
Dinoflagellates (Dinophyceae)	*Akashiwo sanguinea* (Hirasaka) Hansen & Moestrup			X			
	Alexandrium sp.	1.1					9.8
	Amphidinium spp.		2.9		1.1		3.7
	Dinophysis acuminata Claparède & Lachmann			X			
	Ensiculifera sp.					X	
	Gymnodinium spp.	12.8	20.0	132.6	13.9	94.1	107.5
	Gyrodinium lachryma (Meunier) Kofoid & Swezy[*]	1.1					
	Gyrodinium spp.	1.1		8.6			8.6
	Lebouridinium glaucum (Lebour) Gomez, Takayama, Moreira & Lopez-Garcia			29.9			
	Polykrikos sp.			4.3			
	Protoperidinium bipes (Paulsen) Balech[*]			4.3		25.7	
	Protoperidinium leonis (Pavillard) Balech[*]			8.6			
	Protoperidinium sp.[*]			8.6			
	Pyrophacus cf. *horologium*			X			
	Scrippsiella acuminata (Ehrenberg) Kretschmann, Elbrächter, Zinssmeister, S. Soehner, Kirsch, Kusber & Gottschling			12.8		8.6	
Prymnesiophyceae	*Phaeocystis* spp. (single cells)			4460			
Unidentified flagellates/coccoids 2–8 μm	2–5 μm	110.1	627.1	2134	114.4	1032	1586
	5–8 μm	31.0	20.0	21.4	36.3	909.3	129.5
Cryptomonads (Cryptophyceae)	Cryptomonad cells		5.7	218.1		51.3	44.0
Prasinophyceae	*Pyramimonas* cf. *nansenii*	1.1					
	Pyramimonas spp.					20.0	163.7
Chrysophyceae	*Dinobryon balticum* (Schütt) Lemmermann	62.0	2.9				6.1
	Dinobryon sp.					116.9	
	Unidentified cysts					X	
Euglenophyceae	*Eutreptiella* sp.	12.8		17.1			
	Unidentified cells			17.1		X	
Chlorophyceae	*Chlamydomonas* sp.						2.4
Unidentified	Unidentified cells	4.3	5.7				

References

Ardyna, M., Gosselin, M., Michel, C., Poulin, M., Tremblay, J.-É., 2011. Environmental forcing of phytoplankton community structure and function in the Canadian High Arctic: contrasting oligotrophic and eutrophic regions. Mar. Ecol. Prog. Ser. 442, 37–57. http://dx.doi.org/10.3354/meps09378.

Baines, S.B., Twining, B.S., Brzezinski, M.A., Nelson, D.M., Fisher, N.S., 2010. Causes and biogeochemical implications of regional differences in silicification of marine diatoms. Global Biogeochem. Cycles 24, GB4031. http://dx.doi.org/10.1029/2010GB003856.

Balzano, S., Marie, D., Gourvil, P., Vaulot, D., 2012. Composition of the summer photosynthetic pico and nanoplankton communities in the Beaufort Sea assessed by T-RFLP and sequences of the 18S rRNA gene from flow cytometry sorted samples. The ISME J. 6, 1480–1498. http://dx.doi.org/10.1038/ismej.2011.213.

Bergeron, M., Tremblay, J.-É., 2014. Shifts in biological productivity inferred from nutrient drawdown in the southern Beaufort Sea (2003–2011) and northern Baffin Bay (1997–2011), Canadian Arctic. Geophys. Res. Lett. 41, 3979–3987. http://dx.doi.org/10.1002/2014GL059649.

Booth, B.C., 1987. The use of autofluorescence for analyzing oceanic phytoplankton communities. Bot. Mar. 30, 101–108.

Booth, B.C., 1988. Size classes and major taxonomic groups of phytoplankton at two locations in the subarctic Pacific Ocean in May and August, 1984. Mar. Biol. 97, 275–286.

Booth, B.C., Lewin, J., Postel, J.R., 1993. Temporal variation in the structure of autotrophic and heterotrophic communities in the subarctic Pacific. Prog. Oceanogr. 32,

57–99.

Booth, B.C., Horner, R.A., 1997. Microalgae on the Arctic Ocean section, 1994: species abundance and biomass. Deep-Sea Research II 44 (8), 1607–1622.

Booth, B.C., Smith, W.O., 1997. Autotrophic flagellates and diatoms in the Northeast Water Polynya, Greenland: summer 1993. J. Mar. Syst. 10, 241–261.

Boyd, P.W., Muggli, D.L., Varela, D.E., Goldblatt, R.H., Chretien, R., Orians, K.J., Harrison, P.J., 1996. In vitro iron enrichment in the NE subarctic Pacific. Mar. Ecol. Prog. Ser. 136, 179–193.

Boyd, P.W., et al., 2004. The decline and fate of an iron-induced subarctic phytoplankton bloom. Nature 428 (6982), 549–553. http://dx.doi.org/10.1038/nature02437.

Brzezinski, M.A., 1985. The Si:C: N ratio of marine diatoms: interspecific variability and the effect of some environmental variables. J. Phycol. 21, 347–357.

Carmack, E., Wassmann, P., 2006. Food webs and physical–biological coupling on pan-Arctic shelves: unifying concepts and comprehensive perspectives. Prog. Oceanogr. 71, 446–477. http://dx.doi.org/10.1016/j.pocean.2006.10.004.

Carmack, E., McLaughlin, F., 2011. Towards recognition of physical and geochemical change in Subarctic and Arctic Seas. Prog. Oceanogr. 90 (1–4), 90–104. http://dx.doi.org/10.1016/j.pocean.2011.02.007.

Chamnansinp, A., Li, Y., Lundholm, N., Moestrup, Ø., 2013. Global diversity of two widespread, colony-forming diatoms of the marine plankton, *Chaetoceros socialis* (syn. *C. radians*) and *Chaetoceros gelidus* sp. nov. J. Phycol. 49, 1128–1141. http://dx.doi.org/10.1111/jpy.12121.

Codispoti, L.A., Kelly, V., Thessen, A., Matrai, P., Suttles, S., Hill, V., Steele, M., Light, B., 2013. Synthesis of primary production in the Arctic Ocean: III. Nitrate and phosphate based estimates of net community production. Prog. Oceanogr. 110, 126–150. http://dx.doi.org/10.1016/j.pocean.2012.11.006.

Coupel, P., Jin, H.Y., Joo, M., Horner, R., Bouvet, H.A., Sicre, M.-A., Gascard, J.-C., Chen, J.F., Garçon, V., Ruiz-Pino, D., 2012. Phytoplankton distribution in unusually low sea ice cover over the Pacific Arctic. Biogeosciences 9, 4835–4850. http://dx.doi.org/10.5194/bg-9-4835-2012.

Coupel, P., Matsuoka, A., Ruiz-Pino, D., Gosselin, M., Marie, D., Tremblay, J.-É., Babin, M., 2015. Pigment signatures of phytoplankton communities in the Beaufort Sea. Biogeosciences 12, 991–1006. http://dx.doi.org/10.5194/bg-12-991-2015.

Crawford, D.W., Wyatt, S.N., Wrohan, I.A., Cefarelli, A.O., Giesbrecht, K.E., Kelly, B., Varela, D.E., 2015. Low particulate carbon to nitrogen ratios in marine surface waters of the Arctic. Global Biogeochem. Cycles 29, 2021–2033. http://dx.doi.org/10.1002/2015GB005200.

Degerlund, M., Huseby, S., Zingone, A., Sarno, D., Landfald, B., 2012. Functional diversity in cryptic species of *Chaetoceros socialis* Lauder (Bacillariophyceae). J. Plankton Res. 34 (5), 416–431. http://dx.doi.org/10.1093/plankt/fbs004.

Ferrario, M., Sar, E., Sala, S., 1995. Metodologia basica para el studio del fitoplancton con especial referencia a las diatomeas. In: Alveal, K., Ferrario, M.E., Oliverira, E.C., Sar, E. (Eds.), Manual de Métodos Ficológicos. Universidad de Concepción, Concepción, Chile.

Fragoso, G.M., Poulton, A.J., Yashayaev, I.M., Head, E.J.H., Stinchcombe, M.C., Purdie, D.A., 2016. Biogeographical patterns and environmental controls of phytoplankton communities from contrasting hydrographical zones of the Labrador Sea. Prog. Oceanogr. 141, 212–226. http://dx.doi.org/10.1016/j.pocean.2015.12.007.

Fragoso, G.M., Poulton, A.J., Yashayaev, I.M., Head, E.J.H., Purdie, D.A., 2017. Spring phytoplankton communities of the Labrador Sea (2005–2014): pigment signatures, photophysiology and elemental ratios. Biogeosciences 14, 1235–1259. http://dx.doi.org/10.5194/bg-2016-295.

Gaonkar, C.C., Kooistra, W.H.C.F., Lange, C.B., Montresor, M., Sarno, D., 2017. Two new species in the *Chaetoceros socialis* complex (Bacillariophyta): *C. sporotruncatus* and *C. dichatoensis*, and characterization of its relatives, *C. radicans* and *C. cinctus*. J. Phycol. 53, 889–907. http://dx.doi.org/10.1111/jpy.12554.

Garneau, M.E., Gosselin, M., Klein, B., Tremblay, J.-É., Fouilland, E., 2007. New and regenerated production during a late summer bloom in an Arctic polynya. Mar. Ecol. Prog. Ser. 345, 13–26. http://dx.doi.org/10.3354/meps06965.

Geider, R.J., 1987. Light and temperature dependence of the carbon to chlorophyll *a* ratio in microalgae and cyanobacteria: implications for physiology and growth of phytoplankton. New Phytol. 106, 1–34.

Gosselin, M., Levasseur, M., Wheeler, P.A., Horner, R.A., Booth, B.C., 1997. New measurements of phytoplankton and ice algal production in the Arctic Ocean. Deep-Sea Res. II 44 (8), 1623–1644.

Grebmeier, J.M., Overland, J.E., Moore, S.E., Farley, E.V., Carmack, E.C., Cooper, L.W., Frey, K.E., Helle, J.H., McLaughlin, F.A., McNutt, S.L., 2006. A major ecosystem shift in the northern Bering Sea. Science 311, 1461–1464. http://dx.doi.org/10.1126/science.1121365.

Harrison, P.J., 2002. Station Papa time series: insights into ecosystem dynamics. J. Oceanogr. 58, 259–264.

Hasle, G.R., Fryxell, G.A., 1970. Diatoms: cleaning and mounting for light and electron microscopy. Trans. Am. Microscopical Soc. 89 (4), 469–474.

Hill, V., Cota, G., Stockwell, D., 2005. Spring and summer phytoplankton communities in the Chukchi and Eastern Beaufort Seas. Deep-Sea Res. II 52, 3369–3385. http://dx.doi.org/10.1016/j.dsr2.2005.10.010.

Hill, V.J., Matrai, P.A., Olson, E., Suttles, S., Steele, M., Codispoti, L.A., Zimmerman, R.C., 2013. Synthesis of integrated primary production in the Arctic Ocean: II. In situ and remotely sensed estimates. Prog. Oceanogr. 110, 107–125. http://dx.doi.org/10.1016/j.pocean.2012.11.005.

Hill, V., Ardyna, M., Lee, S.-H., Varela, D.E., 2017. Decadal trends in phytoplankton production in the Pacific Arctic Region from 1950 to 2012. Deep-Sea Res. II. http://dx.doi.org/10.1016/j.dsr2.2016.12.015.

Hillebrand, H., Dürselen, C.-D., Kirschtel, D., Pollingher, U., Zohary, T., 1999. Biovolume calculation for pelagic and benthic microalgae. J. Phycol. 35, 403–424.

Horner, R.A., 2002. A Taxonomic Guide to Some Common Marine Phytoplankton. Biopress Limited, Bristol, England.

Joo, H.M., Lee, S.H., Jung, S.W., Dahms, H.-U., Lee, J.H., 2012. Latitudinal variation of phytoplankton communities in the western Arctic Ocean. Deep-Sea Res. II 81–84, 3–17. http://dx.doi.org/10.1016/j.dsr2.2011.06.004.

Kirchman, D.L., Hill, V., Cottrell, M.T., Gradinger, R., Malmstrom, R.R., Parker, A., 2009. Standing stocks, production, and respiration of phytoplankton and heterotrophic bacteria in the western Arctic Ocean. Deep-Sea Res. II 56, 1237–1248. http://dx.doi.org/10.1016/j.dsr2.2008.10.018.

Krause, J.W., Brzezinski, M.A., Landry, M.R., Baines, S.B., Nelson, D.M., Selph, K.E., Taylor, A.G., Twining, B.S., 2010. The effects of biogenic silica detritus, zooplankton grazing, and diatom size structure on silicon cycling in the euphotic zone of the eastern equatorial Pacific. Limnol. Oceanogr. 55 (6), 2608–2622. http://dx.doi.org/10.4319/lo2010.55.6.2608.

Kubiszyn, A.M., Wiktor, J.M., Wiktor Jr., J.M., Griffiths, C., Kristiansen, S., Gabrielsen, T.M., 2017. The annual planktonic protist community structure in an ice-free high Arctic fjord (Adventfjorden, West Spitsbergen). J. Mar. Syst. 169, 61–72. http://dx.doi.org/10.1016/j.jmarsys.2017.01.013.

Li, W.K.W., McLaughlin, F.A., Lovejoy, C., Carmack, E.C., 2009. Smallest algae thrive as the Arctic Ocean freshens. Science 326, 539. http://dx.doi.org/10.1126/science.1179798.

Lovejoy, C., Vincent, W.F., Bonilla, S., Roy, S., Martineau, M.-J., Terrado, R., Potvin, M., Massana, R., Pedrós-Alió, C., 2007. Distribution, phylogeny, and growth of cold-adapted picoprasinophytes in Arctic seas. J. Phycol. 43, 78–89. http://dx.doi.org/10.1111/j.1529-8817.2006.00310.x.

Lovejoy, C., Galand, P.E., Kirchman, D.L., 2011. Picoplankton diversity in the Arctic Ocean and surrounding seas. Mar. Biodivers. 41, 5–12. http://dx.doi.org/10.1007/s12526-010-0062-z.

Lovejoy, C., Potvin, M., 2011. Microbial eukaryotic distribution in a dynamic Beaufort Sea and the Arctic Ocean. J. Plankton Res. 33 (3), 431–444. http://dx.doi.org/10.1093/plankt/fbq124.

Martin, J., Tremblay, J.-É., Price, N.M., 2012. Nutritive and photosynthetic ecology of subsurface chlorophyll maxima in Canadian Arctic waters. Biogeosciences 9, 5353–5371. http://dx.doi.org/10.5194/bg-9-5353-2012.

Matrai, P.A., Olson, E., Suttles, S., Hill, V., Codispoti, L.A., Light, B., Steele, M., 2013. Synthesis of primary production in the Arctic Ocean: I. Surface waters, 1954–2007. Prog. Oceanogr. 110, 93–106. http://dx.doi.org/10.1016/j.pocean.2012.11.004.

McLaughlin, F.A., Carmack, E.C., 2010. Deepening of the nutricline and chlorophyll maximum in the Canada Basin interior, 2003–2009. Geophys. Res. Lett. 37, L24602. http://dx.doi.org/10.1029/2010GL045459.

Menden-Deuer, S., Lessard, E.J., 2000. Carbon to volume relationships for dinoflagellates, diatoms, and other protist plankton. Limnol. Oceanogr. 45 (3), 569–579.

Montagnes, D.J.S., Berges, J.A., Harrison, P.J., Taylor, F.J.R., 1994. Estimating carbon, nitrogen, protein, and chlorophyll *a* from volume in marine phytoplankton. Limnol. Oceanogr. 39 (5), 1044–1060.

Mostajir, B., Gosselin, M., Gratton, Y., Booth, B., Vasseur, C., Garneau, M.-È., Fouilland, É., Vidussi, F., Demers, S., 2001. Surface water distribution of pico- and nanophytoplankton in relation to two distinctive water masses in the North Water, northern Baffin Bay, during fall. Aquat. Microb. Ecol. 23, 205–212.

Parsons, T.R., Maita, Y., Lalli, C.M., 1984. A Manual of Biological and Chemical Methods for Seawater Analysis. Pergamon, Oxford, U. K.

Peña, M.A., Varela, D.E., 2007. Seasonal and interannual variability in phytoplankton and nutrient dynamics along Line P in the NE subarctic Pacific. Prog. Oceanogr. 75 (2), 200–222. http://dx.doi.org/10.1016/j.pocean.2007.08.009.

Poulin, M., Daugbjerg, N., Gradinger, R., Ilyash, L., Ratkova, T., von Quillfeldt, C., 2011. The pan-Arctic biodiversity of marine pelagic and sea-ice unicellular eukaryotes: a first-attempt assessment. Mar. Biodivers. 41, 13–28. http://dx.doi.org/10.1007/s12526-010-0058-8.

Schloss, I.R., Nozais, C., Mas, S., van Hardenberg, B., Carmack, E., Tremblay, J.-É., Brugel, S., Demers, S., 2008. Picophytoplankton and nanophytoplankton abundance and distribution in the southeastern Beaufort Sea (Mackenzie Shelf and Amundsen Gulf) during Fall 2002. J. Mar. Syst. 74, 978–993.

Sherr, E.B., Sherr, B.F., Fessenden, L., 1997. Heterotrophic protists in the Central Arctic Ocean. Deep-Sea Res. II 44 (8), 1665–1682.

Sherr, E.B., Sherr, B.F., Wheeler, P.A., Thompson, K., 2003. Temporal and spatial variation in stocks of autotrophic and heterotrophic microbes in the upper water column of the central Arctic Ocean. Deep-Sea Research I 50, 557–571. http://dx.doi.org/10.1016/S0967-0637(03)00031-1.

Smith, W.O., Sakshaug, E., 1990. Polar Phytoplankton. In: Smith, W.O. (Ed.), Polar Oceanography, Part B. Academic, San Diego, CA, pp. 477–525.

Sukhanova, I.N., Flint, M.V., Pautova, L.A., Stockwell, D.A., Grebmeier, J.M., Sergeeva, V.M., 2009. Phytoplankton of the western Arctic in the spring and summer of 2002: structure and seasonal changes. Deep-Sea Res. II 56, 1223–1236. http://dx.doi.org/10.1016/j.dsr2.2008.12.030.

Taylor, A.H., Geider, R.J., Gilbert, F.J.H., 1997. Seasonal and latitudinal dependencies of phytoplankton carbon-to-chlorophyll *a* ratios: results of a modelling study. Mar. Ecol. Prog. Ser. 152, 51–66.

Taylor, R.L., Semeniuk, D.M., Payne, C.D., Zhou, J., Tremblay, J.-É., Cullen, J.T., Maldonado, M.T., 2013. Colimitation by light, nitrate, and iron in the Beaufort Sea in late summer. J. Geophys. Res. Oceans 118, 3260–3277. http://dx.doi.org/10.1002/jgrc.20244.

Tomas, C.R., 1997. Identifying Marine Phytoplankton. Academic Press, San Diego, pp. 858.

Tremblay, J.-É., Gratton, Y., Fauchot, J., Price, N.M., 2002. Climatic and oceanic forcing of new, net, and diatom production in the North Water. Deep Sea Res. Part II 49, 4927–4946. http://dx.doi.org/10.1016/S0967-0645(02)00171-6.

Tremblay, G., Belzile, C., Gosselin, M., Poulin, M., Roy, S., Tremblay, J.-É., 2009. Late

summer phytoplankton distribution along a 3500 km transect in Canadian Arctic waters: strong numerical dominance by picoeukaryotes. Aquat. Microb. Ecol. 54, 55–70. http://dx.doi.org/10.3354/ame01257.

Tremblay, J.-É., Bélanger, S., Barber, D.G., Asplin, M., Martin, J., Darnis, G., Fortier, L., Gratton, Y., Link, H., Archambault, P., Sallon, A., Michel, C., Williams, W.J., Philippe, B., Gosselin, M., 2011. Climate forcing multiplies biological productivity in the coastal Arctic Ocean. Geophys. Res. Lett. 38, L18604. http://dx.doi.org/10.1029/2011GL048825.

Utermöhl, H., 1958. Zur Vervollkommnung der quantitativen Phytoplankton-Methodik. Internationale Vereinigung für Theoretische und Angewandte Limnologie. Komitee für Limnologische Methoden. 9, 1–39.

Varela, D.E., Crawford, D.W., Wrohan, I.A., Wyatt, S.N., Carmack, E.C., 2013. Pelagic primary productivity and upper ocean nutrient dynamics across Subarctic and Arctic Seas. J. Geophys. Res. Oceans 118, 7132–7152. http://dx.doi.org/10.1002/2013JC009211.

Varela, D.E., Harrison, P.J., 1999. Seasonal variability in nitrogenous nutrition of phytoplankton assemblages in the northeastern subarctic Pacific Ocean. Deep-Sea Res. II 46 (11–12), 2505–2538. http://dx.doi.org/10.1016/S0967-0645(99)00074-0.

Vidussi, F., Roy, S., Lovejoy, C., Gammelgaard, M., Thomsen, A.H., Booth, B., Tremblay, J.-É., Mostajir, B., 2004. Spatial and temporal variability of the phytoplankton community structure in the North Water Polynya, investigated using pigment biomarkers. Can. J. Fish. Aquat. Sci. 61, 2038–2052. http://dx.doi.org/10.1139/F04-152.

Walsh, J.J., McRoy, C.P., Coachman, L.K., Goering, J.J., Nihoul, J.J., Whitledge, T.E., Blackburn, T.H., Springer, A.M., Tripp, R.D., Hansell, D.A., Djenidi, S., Deleersnijder, E., Henriksen, K., Lund, B.A., Andersen, P., Muller-Karger, F.E., Dean, K.K., 1989. Carbon and nitrogen cycling within the Bering/Chukchi Seas: source regions for organic matter effecting AOU demands of the Arctic Ocean. Prog. Oceanogr. 22, 277–359.

Wyatt, S.N., Crawford, D.W., Wrohan, I.A., Varela, D.E., 2013. Distribution and composition of suspended biogenic particles in surface waters across Subarctic and Arctic Seas. J. Geophys. Res. Oceans 118, 6867–6880. http://dx.doi.org/10.1002/2013JC009214.

Yamamoto-Kawai, M., Carmack, E., McLaughlin, F., 2006. Nitrogen balance and arctic throughflow. Nature 443 (7107), 43. http://dx.doi.org/10.1038/443043a.